Since January 2020 Elsevier has created a COVID-19 resource centre with free information in English and Mandarin on the novel coronavirus COVID-19. The COVID-19 resource centre is hosted on Elsevier Connect, the company's public news and information website.

Computers in Biology and Medicine 136 (2021) 104698

Contents lists available at ScienceDirect

Computers in Biology and Medicine

journal homepage: www.elsevier.com/locate/compbiomed

Evolutionary warning system for COVID-19 severity: Colony predation algorithm enhanced extreme learning machine

Beibei Shi [a,1], Hua Ye [b,1], Long Zheng [b], Juncheng Lyu [c], Cheng Chen [d], Ali Asghar Heidari [e,2], Zhongyi Hu [f], Huiling Chen [f,*], Peiliang Wu [g,**]

[a] Affiliated People's Hospital of Jiangsu University, 8 Dianli Road, Zhenjiang, Jiangsu, 212000, China
[b] Department of Pulmonary and Critical Care Medicine, Affiliated Yueqing Hospital, Wenzhou Medical University, Yueqing, 325600, China
[c] Weifang Medical University School of Public Health, China
[d] Center of Clinical Research, Wuxi People's Hospital of Nanjing Medical University, Wuxi, Jiangsu, 214023, China
[e] School of Surveying and Geospatial Engineering, College of Engineering, University of Tehran, Tehran, Iran
[f] College of Computer Science and Artificial Intelligence, Wenzhou University, Wenzhou, 325035, China
[g] Department of Pulmonary and Critical Care Medicine, The First Affiliated Hospital of Wenzhou Medical University, Wenzhou 325000, China

ARTICLE INFO

Keywords:
Coronavirus disease 2019
Biochemical indexes
Colony predation algorithm
Kernel extreme learning machine
Warning system
COVID-19

ABSTRACT

Coronavirus Disease 2019 (COVID-19) was distributed globally at the end of December 2019 due to severe acute respiratory syndrome coronavirus 2 (SARS-CoV-2). Early diagnosis and successful COVID-19 assessment are missing, clinical care is ineffective, and deaths are high. In this study, we investigate whether the level of biochemical indicators helps to discriminate and classify the severity of the COVID-19 using the machine learning method. This research creates an efficient intelligence method for the diagnosis of COVID-19 from the perspective of biochemical indexes. The framework is proposed by integrating an enhanced new stochastic called the colony predation algorithm (CPA) with a kernel extreme learning machine (KELM), abbreviated as ECPA-KELM. The core feature of the approach is the ECPA algorithm which incorporates the two main operators that have been abstained from the grey wolf optimizer and moth-flame optimizer to improve and restore the CPA research functions and are simultaneously used to optimize the parameters and to select features for KELM. The ECPA output is checked thoroughly using IEEE CEC2017 benchmark to verify the capacity of the proposed methodology. Finally, in the diagnosis of COVID-19 using biochemical indexes, the designed ECPA-KELM model and other competing KELM models based on other optimization are used. Checking statistical results will display improved predictive properties for all metrics and higher stability. ECPA-KELM can also be used to discriminate and classify the severity of the COVID-19 as a possible computer-aided method and provide effective early warning for the treatment and diagnosis of COVID-19.

1. Introduction

Coronavirus Disease 2019 (COVID-19) was found to have spread around the world in late December 2019 as a result of severe acute respiratory syndrome coronavirus 2 (SARS-CoV-2) [1,2]. COVID-19 has shown an intensive global spread, and thus the danger to human health is serious. As of June 11, 2020, COVID-19 was responsible for 7,273,958 confirmatory cases worldwide and 413,372 deaths [3]. COVID-19's clinical features may echo other coronavirus diseases, including Severe Acute Respiratory Syndrome Coronavirus (SARS-CoV). Globally, the current human mortality rate for infection with SARS-CoV-2 is 3.4% [4]. However, the mortality rate of serious COVID-19 patients in Wuhan was as high as 10%–40% [5]. Therefore, early and accurate identification of severe COVID-19 patients and rapid assessment of the severity of the

* Corresponding author.
** Corresponding author.
E-mail addresses: shibeibei1993zjfph@163.com (B. Shi), 154671045@qq.com (H. Ye), 7270684@qq.com (L. Zheng), cheng_china@163.com (J. Lyu), chenchnjmu@163.com (C. Chen), as_heidari@ut.ac.ir (A.A. Heidari), huzhongyi@wzu.edu.cn (Z. Hu), chenhuiling.jlu@gmail.com, chenhuiling.jlu@gmail.com (H. Chen), pl_wu@163.com (P. Wu).
[1] These authors contributed equally to this work.
[2] https://aliasgharheidari.com

https://doi.org/10.1016/j.compbiomed.2021.104698
Received 19 May 2021; Received in revised form 20 July 2021; Accepted 23 July 2021
Available online 30 July 2021

disease are important for determining individualized treatment plans for COVID-19 patients and assisting e-healthcare systems [6]. To solve this problem, we have studied cheap and common hematologic markers as indicators of the severity of COVID-19 and poor clinical outcomes. However, it is hard to differentiate between severe COVID-19 patients based on a single indicator from non-severe COVID-19 patients. To do so, we integrate multiple indicators to develop a new prediction model for early recognition and classify the severity of COVID-19.

In recent years, artificial intelligence (AI) has been commonly used in different life sciences [7–11]. For instance, in the field of ophthalmology, the ability of AI to distinguish diseases has reached the level of an expert [12]. AI can assist radiologists to make the qualitative diagnosis of benign and malignant thyroid nodules in the field of radiology [13]. With the rapid development of AI, machine learning (ML) technology has been widely used for diagnosis of disease, developed predictive models assisting clinical decision-making in medical fields, and quickly identified the key factors associated with the diseases [14–17]. Therefore, machine learning-based AI technology is becoming an increasingly indispensable computational tool in the medical field. Similarly, machine learning-based technology has been applied to in disease diagnosis [18]. Computer tomography (CT) or x-ray image recognition [19,20], disease epidemic, surveillance, and control [21,22] in the course of the COVID-19 outbreak. Ebadi et *al.* [23] used multiple sources (PubMed and ArXiv) to define the scene of the current COVID-19 research with multiple learning machines by identifying latent subjects and analyzing the evolution, the similarities between publications, and sentiment of the research topics developed. Three NLP algorithms have been developed to trace positive CT imaging of typical SARS-CoV-2 viral inflammatory diseases [24]. A recent data collection of COVID-19 CT scans, known as COVID-CT-MD, consists not only of COVID-19 cases but also stable and community-acquired pneumonia (CAP) participants that can assist in developing advanced machine learning and DNN solutions [25]. Chowdhury et *al.* [26] developed an early warning method to predict mortality risk in machine learning COVID-19 patients. The random vulnerability model used by the forest machine for the creation of a novel COVID-19 Vulnerability Index (C19VI) [27]. In brief, machine learning can be extremely efficient in the analysis of COVID-19 before diagnosis and disease data.

This research is the first time an evolutionary kernel extreme learning machine is built to diagnose COVID-19 from a biochemical index perspective.

For the first time, a system to diagnose COVID-19 from a biochemical index point of view is designed for an evolutionary kernel extreme learning machine in this study. The two core operators use this proposed method (ECPA-KELM) to improve and re-establish the search capabilities for colony predation algorithm (CPA), abstracted from the Grey Wolf and Moth Flame Optimizers, which can provide for considerable convergence and the potential to spring from the stagnant local population, ECPA is designed to simultaneously perform diagnosis of COVID-19 parameter optimization and selection features of KELM. The ECPA output is first thoroughly verified through IEEE CEC2017 benchmark test cases [28] to verify the capacity of the proposed methodology. Lastly, COVID-19 clinical data was used with biochemical indexes to develop the ECPA-KELM and other competitor KELM models based on other optimization algorithms. By analyzing the experimental findings, the ECPA core compensation is verified, and a solid ECPA-KELM in terms of various performance assessment indexes to determine the COVID-19 status can be achieved. The results of the test showed that the ECPA-KELM proposed was seemingly beneficial.

The key contribution in this analysis is as follows:

- To improve and restore the CPA search capability (ECPA), both core operators have taken away the grey wolf optimizer and moth-flame optimizer.
- The proposed hybrid ECPA has achieved a significant impact on CEC2017 optimization tasks.
- For the first time, the ECPA proposed successfully solved KELM's parameter optimization and feature selection simultaneously.
- An effective ECPA-KELM technique is used to help diagnose COVID-19 from the perspective of biochemical indicators.

The paper was organized accordingly—the materials and procedures described in paragraph 2. The proposed ECPA algorithm is presented in Section 3. Section 4 describes the proposed ECPA-KELM model. Section 5 describes the designs of the experiments. Section 6 displays the results of CEC2017 ECPA and the diagnosis of COVID-19 data set simulations and ECPA-KELM. Section 7 deals with the results. The conclusion and trajectory of the future are shown in Section 8.

2. Methods and materials

2.1. Collecting data

The study included COVID-19 patients at Wenzhou Medical University affiliated Yueqing Hospital, Wenzhou, China. The research was accepted by the Ethics Committee of affiliated Yueqing Hospital, Wenzhou Medical University (No. 202000002 Ethics), and by all COVID-19 patients, an informed consent document was signed. A total of 51 COVID-19 patients were included in the analysis in retrospect between January 21 and March 20, 2020. For each COVID-19 patient, information on gender, age, biochemical index, and blood electrolyte was collected. Biochemical indexes and blood electrolytes were determined using an automated biochemical analyzer (BS-190; Mindray, Shenzhen, China) in the laboratory of clinical biochemistry, the Affiliated Yueqing Hospital of Wenzhou Medical University.

In our research, COVID-19 was diagnosed based on criteria developed by the Peoples' Republic of China National Health Commission. Once the diagnosis of COVID-19 was confirmed, we divided patients into four categories according to the clinical manifestations: mild, general, severe, and critically ill patients. Clinical characteristics of mild COVID-19 patients include no symptoms or mild symptoms, no lung involvement. Clinical characteristics of general COVID-19 patients include respiratory symptoms (fever, dry cough, fatigue, nose congestion, runny nose, sore throat), gastrointestinal symptoms (nausea, vomiting, diarrhea), and pulmonary disease SARS-CoV-2. Clinical criteria for severe COVID-19 patients include at least one of the following: a) patient exhibit dyspnea and respiratory rate $\geq$30 breaths/minute; b) the levels of blood oxygen saturation $\leq$93%; c) the oxygenation index (OI) $\leq$ 300 mmHg. Clinical criteria for critically ill COVID-19 patients include at least one of the following: a) patient develop acute respiratory failure requiring mechanical ventilation; b) patient develop shock; c) patient present with multiple organ failure requiring treatment in an intensive care unit (ICU). Mild, general COVID-19 patients were categorized into one group and named non-severe COVID-19 group, and severe, critically ill patients were categorized into one group and named severe COVID-19 group.

2.2. Statistical results

Statistical analysis using SPSS software was performed. Age, biochemical index, and blood electrolyte comparison were tested using an independent-samples *t*-test between the non-severe COVID-19 and severe COVID-19 groups. Age, biochemical index, and blood electrolyte are presented as mean $\pm$ standard deviation ($\overline{x} \pm SD$) for continuous variables. The patient information, biochemical index, and blood electrolyte of COVID-19 patients have listed in Table 1. The statistical results of age, biochemical index, and blood electrolyte were shown in Table 2.

2.3. Colony predation algorithm (CPA)

Optimization methods, in addition to other cases in healthcare systems, have found their value and obtained great attention in many fields

Table 1
List of characteristics and meanings used in this analysis.

No.	Feature	Abbreviation
F1	Gender	Gender
F2	Age	Age
F3	Total bilirubin	TBIL
F4	Direct bilirubin	DBIL
F5	Alanine aminotransferase	ALT
F6	Total protein	TP
F7	Albumin	ALB
F8	Globulin	GLB
F9	Albumin/Globulin ratio	A/G
F10	Alkaline phosphatase	ALP
F11	Gamma-Glutamyltransferase	GGT
F12	Aspartate aminotransferase	AST
F13	Creatine kinase	CK
F14	Lactate dehydrogenase	LDH
F15	Creatine kinase isoenzymes	CK-MB
F16	Potassium ion	K^+
F17	Sodium ion	Na^+
F18	Chloride ion	Cl^-
F19	Blood urea nitrogen	BUN
F20	Creatinine	Cr
F21	Uric acid	UA
F22	Inorganic phosphorus	P^+
F23	Blood magnesium	Mg^{2+}
F24	Calcium ion	Ca^{2+}
F25	Troponin I	TnI

Table 2
Biochemical index & blood electrolyte in non-severe group and severe group.

Index	Non-severe group (n = 30)	Severe group (n = 21)	p-value
Age (years)	42.30 ± 11.53	61.43 ± 17.64	0.000
TBIL (umol/l)	10.42 ± 6.42	12.37 ± 8.46	0.353
DBIL (umol/l)	4.76 ± 1.63	7.68 ± 4.93	0.015
ALT (u/l)	23.33 ± 14.62	63.62 ± 79.34	0.032
TP (g/l)	66.65 ± 4.33	67.86 ± 7.68	0.520
ALB (g/l)	41.53 ± 2.57	35.90 ± 4.65	0.000
GLB (g/l)	25.13 ± 3.28	31.97 ± 7.27	0.000
A/G	1.68 ± 0.24	1.19 ± 0.36	0.000
ALP(u/l)	61.17 ± 15.57	71.24 ± 27.63	0.142
GGT(u/l)	36.83 ± 29.79	90.00 ± 99.97	0.027
AST(u/l)	23.13 ± 7.62	65.43 ± 51.08	0.001
CK(u/l)	76.27 ± 45.22	246.52 ± 300.47	0.018
LDH(u/l)	244.37 ± 61.07	382.95 ± 152.78	0.001
CK-MB(u/l)	21.23 ± 9.08	19.76 ± 8.44	0.561
K^+(mmol/l)	4.23 ± 0.48	4.07 ± 0.62	0.291
Na^+(mmol/l)	139.26 ± 1.96	133.84 ± 4.02	0.000
Cl^-(mmol/l)	100.19 ± 2.92	95.55 ± 3.39	0.000
BUN(mmol/l)	3.71 ± 0.99	4.64 ± 1.98	0.057
Cr(umol/l)	60.57 ± 12.29	70.29 ± 15.88	0.017
UA(umol/l)	264.83 ± 69.15	210.33 ± 87.73	0.017
P^+(mmol/l)	1.01 ± 0.17	0.95 ± 0.25	0.339
Mg^{2+}(mmol/l)	0.91 ± 0.07	0.93 ± 0.09	0.472
Ca^{2+}(mmol/l)	2.19 ± 0.07	2.08 ± 0.09	0.000
TnI(ng/ml)	0.01 ± 0.01	0.29 ± 1.19	0.292

such as scheduling problems [29,30], image segmentation [31,32], fault diagnosis of rolling bearings [33,34], bankruptcy prediction [35–37], wind speed prediction [38], engineering design problems [39–42]. Also, they have shown more variety of potentials in the hard maximum satisfiability problem [43,44], parameter optimization [45–48], PID optimization control [49–51], gate resource allocation [52,53], feature selection [54–58], medical data classification [59–62], detection of foreign fiber in cotton [63,64], and prediction problems in educational field [65–69]. One of the recent methods is CPA. Like other swarm-based methods [168–170], the dominant idea of CPA is the predation process and predation strategy of group of hunting animals. The algorithm mimics the supportive behavior of social animals and the characteristics of selective hunting. Thus this algorithm is based on the coexistence of social animals. The main steps are composed of communication and collaboration, disperse food, encircle food, supporting closest individual, and searching for the food. The following formulas represent individual cooperative communication and food searching behavior:

$$\vec{X}_j^i(t+1) = r\cdot\vec{X}_j^{i_1}(t) + (1-r)\cdot((\vec{X}_1(t)+\vec{X}_2(t))/2) \tag{1}$$

where r is in the range of [0,1], $\vec{X}_j^{i_1}(t)$ is the individual looking for food, $\vec{X}_1$ and $\vec{X}_2$ are the two closest to prey in the j-th dimension, $j \in 1, 2, \ldots, dim$, $\vec{X}_j^i(t+1)$ is the latest updated position of the individual. Here, the predation strategy displayed by individuals in search is simulated mathematically as $\vec{X}(t+1) = \vec{X}_{best} - S\cdot(r_1(ub-lb)+lb)$, where $\vec{X}(t+1)$ is the position of a population and $\vec{X}_{best}$ is the position of food, S represents the strength of prey, and its absolute value decreases from a to 0 with the number of evaluations, r_1 is the $[R_1; R_2; R_3; \ldots R_j]$, j = dim represents the dimension of the population, ub, and lb represent the upper and lower bounds. It should be noted that S is as follows:

$$S_0 = a - t\cdot\left(\frac{a}{N}\right) S = 2\cdot S_0\cdot r_2 - S_0 \tag{2}$$

where N is the number of individuals, S_0 decreases from a to 0 with the number of evaluations and t represents the current number of evaluations, r_2 is a random number of [0,1].

The hunting group will surround the single prey and keep approaching the prey. This stage can be represented by mathematical simulation as follows:

$$\vec{X}(t+1) = \vec{X}_{best} - 2\cdot S\cdot D\cdot e^l\cdot\tan\left(l\cdot\frac{\pi}{4}\right) \tag{3}$$

where D is the distance between the current individual and the prey as $D = \left|\vec{X}_{best} - \vec{X}(t)\right|$. Mathematical formulaes describe the probabilities of implementing these two predatory strategies as below:

$$\vec{X}(t+1) = \begin{cases} \vec{X}_{best} - S\cdot(r_1\cdot(ub-lb)+lb)\, r_2 \geq 0.5 \\ \vec{X}_{best} - 2\cdot S\cdot D\cdot e^l\cdot\tan\left(l\cdot\frac{\pi}{4}\right) r_2 < 0.5 \end{cases} \tag{4}$$

since the group can experience problems in hunting beasts, the closest person calls for peer help. In mathematical formulas, its policy can be expressed as $\vec{X}(t+1) = \vec{P}_{nearest}$, where $\vec{P}_{nearest}$ nearest is the location of the nearest predator in the support group, $\vec{P}$ is the predator near the prey nearby. The searching for the food can be as:

$$D_1 = abs\left(2\cdot r_4\cdot\vec{X}_{rand} - \vec{X}(t)\right)\vec{X}(t+1) = \vec{X}_{rand} - S\cdot D_1 \tag{5}$$

where D_1 denotes the distance of random group movement, r_4 is a random number of [0,1], and $\vec{X}_{rand}$ is a new individual position formed randomly by individuals. See original paper for detailed details [70].

2.4. Two core operators to be introduced

One core operator is a grey wolf optimizer consisting of social hier-

archy, surrounding beasts, hunting, attacking prey and searching for projection pieces. The key concept is the use of hierarchy. This is the core mathematical model:

$$\vec{D}_\alpha = |\vec{C}_1 \cdot \vec{X}_\alpha - \vec{X}|, \quad \vec{D}_\beta = |\vec{C}_2 \cdot \vec{X}_\beta - \vec{X}|, \quad \vec{D}_\delta = |\vec{C}_3 \cdot \vec{X}_\delta - \vec{X}| \tag{6}$$

Where the $\vec{D}$ means the distance from the prey to the grey wolves, $\vec{A}$ and $\vec{C}$ are vectors of the coefficient $\vec{A} = 2\vec{a} \cdot \vec{r}_1 - \vec{a}$ and $\vec{C} = 2 \cdot \vec{r}_2$, $\vec{X}_\alpha$, $\vec{X}_\beta$ and $\vec{X}_\delta$ are three wolves nearest to the current prey, the t represents the present version. You may refer to more info [71].

$$\vec{X}_1 = \vec{X}_\alpha - \vec{A}_1 \cdot (\vec{D}_\alpha), \quad \vec{X}_2 = \vec{X}_\beta - \vec{A}_2 \cdot (\vec{D}_\beta), \quad \vec{X}_3 = \vec{X}_\delta - \vec{A}_3 \cdot (\vec{D}_\delta) \tag{7}$$

$$\frac{\vec{X}(t+1) = \vec{X}_1 + \vec{X}_2 + \vec{X}_3}{3} \tag{8}$$

Another core operator is a moth-flame.

Another main operator is the moth-flames optimization (MFO) [72]. The location of each moth is changed to a flame with the following equation in order to mathematically model the conduct of moths: $M_i = S(M_i F_j)$, where M_i is the i*th* moth, F_j means the j*th* flame, and S is the spiral function. For the MFO algorithm, a logarithmic spiral is described below:

$$S(M_i, F_j) = D_i \cdot e^{bt} \cdot \cos(2\pi t) + F_j \tag{9}$$

where D_i specifies the i*th* moth distance for the j*th* flame, b is a logarithmic spiral constant for determining the form, and t is a [1,1] random number, D is obtained as $D_i = |F_j - M_i|$, where M_i indicates the i*th* moth, F_j indicates the j*th* flame, and D_i is the distance of the i*th* moth for the j*th* flame. More detailed information can be seen in Ref. [72].

2.5. Brief introduction of kernel extreme learn machine (KELM)

Extreme learning machine (ELM) [73] can learn fast and has very few adjustments parameters, and does not provide the option of input weights and secret preconditions as the latest learning algae to feed-forward neural networks in a single hidden layer. The new theory for an extreme learning machine from the kernel has recently been extended (KELM) [74]. The following is a short overview of the KELM method:

Training set as $A = \{(x_i, t_i) | x_i \in R^n, t_i \in R^m, k = 1, 2, \ldots, N\}$ is given, where n × 1 input feature vector of x_i and m × 1 of t_i target vector. an activation function $h(x)$ can be modeled as follows:

$$\sum_{i=1}^{\widetilde{N}} \beta_i h(w_i \cdot x_j + b_i) = o_j, j = 1, 2, \ldots, N \tag{10}$$

the w_i is the weight vector between the hidden layer of the i*th* and the input layer, and the distinctiveness between the hidden layer of the i*th* is called b_i, the weight vector between the i*th* and the output layer is β_i; o_j is the target vector of the j*th* input data. $w_i \cdot x_j$ is the outcome of the w_i and x_j internal product. The $\widetilde{N}$ means the number of the hidden layer nodes. To assess these samples correctly, $\sum_j^N \|o_j - t_j\| = 0$ is given and $\sum_{i=1}^{\widetilde{N}} \beta_i h(w_i \cdot x_j + b_i) = t_j, j = 1, 2, \ldots, N$ with β_i, w_i, b_i, which can be given as $H\beta = T$, where

$$H(w_1, \ldots, w_{\widetilde{N}}, b_1, \ldots, b_{\widetilde{N}}, x_1, \ldots, x_N) = \begin{pmatrix} h(w \cdot x_1 + b_1) & \cdots & h(w_{\widetilde{N}} \cdot x_1 + b_{\widetilde{N}}) \\ \vdots & \ddots & \vdots \\ h(w \cdot x_N + b_1) & \cdots & h(w_{\widetilde{N}} \cdot x_N + b_{\widetilde{N}}) \end{pmatrix}_{N \times \widetilde{N}} \tag{11}$$

$$\beta = \begin{bmatrix} \beta_1^T \\ \vdots \\ \beta_{\widetilde{N}}^T \end{bmatrix}_{\widetilde{N} \times \mathrm{m}}, T = \begin{bmatrix} \mathrm{t}_1^T \\ \vdots \\ \mathrm{t}_N^T \end{bmatrix}_{N \times \mathrm{m}} \tag{12}$$

H is the result matrix of the hidden layer neural network, with the i*th* column of H being the i*th* hidden output neuron with respect to x_1, x_2, …, x_N. Enter weights and vector secret layer bias need not be adjusted. On this basis, the output weight of the linear system $H\beta = T$ can be given mathematically with the least square solution $\widehat{\beta}$:

$$|H(w_1, \ldots, w_{\widetilde{N}}, b_1, \ldots, b_{\widetilde{N}})\widehat{\beta} - T\| = min_\beta \|H(w_1, \ldots, w_{\widetilde{N}}, b_1, \ldots, b_{\widetilde{N}})\beta - T\| \tag{13}$$

according to the Moore–Penrose (MP) generalized inverse and the kernel learning theory, the output function of KELM is shown as follows:

$$F(x) = h\beta = h(x)H^\dagger(\frac{1}{C} + HH^\dagger)^{-1}T = \begin{bmatrix} K(x, x_1) \\ \vdots \\ K(x, x_N) \end{bmatrix} (\frac{1}{C} + \Omega_{ELM})^{-1}T \tag{14}$$

Usually radial basis function kernel are used in this models as $K(x, x_i) = \exp(-\gamma\|x - x_i\|^2)$, the penalty parameter C and gamma kernel μ are the two main parameters, based on the definitions above. The first parameter C can better off the minimization of fitting errors and the complexity of the model. The second parameter, γ, determines the nonlinear projection from the input area to a large space. More detailed information on KELM can be shown in Ref. [74].

3. Proposed ECPA

As we know, in many decision-making fields, algorithms are required to provide an approximate optimal solution [75–77]. For such complex calculation problems, evolutionary computing methods are widely used to solve such problems. Such as, The global algorithm of particle swarm is used to solve gravity abnormality parameters [78], hybrid genetic algorithm for diagnosing heart disease, and fluid logic classification [79]. Among these evolutionary computing algorithms, there are more widely used particle swarm optimization [80], genetic algorithm [81]. Furthermore, recently, several excellent evolutionary calculation methods have been proposed, grasshopper optimization algorithm [82], harris hawks optimization [83], hunger games search [84]. Among all these evolutionary computing algorithms, CPA, as of the most recent participant and Very easy to implement and complete the application, has been proposed by our team [70]. Through strict experimental data statistics and the application of several engineering problems, the algorithm's efficiency has been tested strongly.

In this analysis, ECPA is designed to increase and restore the search capabilities of the original CPA, both core operators abstracted by the grey wolf optimizer and moth-flame optimizer. To the best of our knowledge, the CPA is integrated with multiple efficient operators for the first time. The designed algorithm ECPA can be divided into three parts. The first is to perform the initialization of the search population. The second is to complete the execution of the algorithm operators in the original CPA, and finally, to complete the execution of the introduced operators derived from the other two algorithms. The detailed pseudo-code of the presented algorithm can refer to Algorithm 1.

Algorithm 1. The pseudo code of designed ECPA.

Algorithm 1: The pseudo code of designed ECPA

Input: The number of population size N;
The number of Maximum iteration T;
Output: Best position X_b;
Best fitness value f_{value};
Initialize population randomly $X_i(i = 1, 2, ..., N)$;
begin
g=0;
while $g < T$ **do**
for $(i = 1 : N)$ **do**
Ensure that any particle is within the search range;
Calculate the fitness of all Individuals;
Update the X_b;
Update the S ;
$S_0 = a - t \cdot \left(\frac{a}{N}\right)$; $S = 2 \cdot S_0 \cdot r_2 - S_0$;
Update the a ;
$a = e^{w-2 \cdot w \cdot \left(1-\frac{g}{T}\right)}$;
Update the r_1; **for** $(j = 1 : dim)$ **do**
Update the X_1, X_2, i_1,r;
If rand < g/T $X_i = X_b$;
Calculate the X_j^i by equation (1);
for $(i = 1 : N)$ **do**
Update S,l;
IF $abs(S) < 2 \times a/3$ Calculate the X_i by equation (4);
else
Calculate the X_i by:
$$\vec{X}(t+1) = \begin{cases} \vec{P}_{nearest} abs(r_6) < 1 \\ \vec{X}_{rand} - S \cdot D_1 abs(r_6) > 1 \end{cases}$$
for $(i = 1 : N)$ **do**
Calculate the X_i by equation (6)-(8);
Calculate the fitness of all Individuals;
Update the X_b;
for $(i = 1 : N)$ **do**
Calculate the X_i by equation (9);
Calculate the fitness of all Individuals;
Update the X_b;
$g = g + 1$;
End-Loop;

4. Proposed ECPA-KELM model

In this study, a kernel extreme learning machine driven by hybrid CPA for diagnosing COVID-19 from the perspective of biochemical indicators is proposed (ECPA-KELM). Fig. 1 shows the flow diagram of ECPA-KELM. From this figure, it can be seen that the cross-validation mechanism is employed as the internal 5- and external 10-fold system, respectively, which means the $K_1 = 5$ and $K_2 = 10$ in this study. The detailed data segmentation diagram is as shown in Fig. 2.

The key part of this proposed method is the KELM, which uses the RBF kernel in terms of input space for mapping the aggregate data into a hidden layer space. The entire algorithm method covers the coefficient of penalty C and kernel width γ, and the subset of n features, the first penalty parameter C sets the balance between minimizing fitting error and the complexity in the model, with the second kernel bandwidth γ defining nonlinear input spatial mapping into some high-dimensional space function.

The ECPA algorithm also develops these two parameters and synchronously converts the optimal feature subset, specifically, continuous space, into binary space utilizing the sigmoid function. The feature is considered to be selected if less than 0.5; otherwise, the characteristics would be discarded. Finally, the evolved KELM by ECPA gives an accurate early diagnosis of COVID-19 from the perspective of biochemical indicators.

5. Experimental designs

The experimental section in this analysis consists of two parts. The first step will be to study the efficiency of the proposed ECPA, and the second part will use the proposed ECPA-KELM algorithm for a biochemical indicator diagnosis of COVID-19.

First of all, the efficiency of the proposed ECPA is extensively verified and carried out in comparison with other algorithms on IEEE CEC 2017 benchmark; these benchmarks are shown in Table 3, and also strictly perforce the balance and diversity analysis of the improved ECPA and its original CPA. Several other algorithms, including CPA, CLPSO, DE, PSO, MFO, and GWO, were involved as competitors on the common benchmark. The algorithm parameters are specified concerning the original documents.

The following experimental examined extensively using the suggested ECPA algorithm to optimize a combination of the best parameter and KELM function subset, which is the result ECPA-KELM used for a biochemical indicator diagnosis of COVID-19 on data collection. In terms of ECPA-KELM, several common learning processes were also compared, including original KELM, GWO-KELM, MFO-KELM, PSO-KELM, SVM, and KNN. The two main parameters of [$-2^{\wedge 5}$, $2^{\wedge 5}$] and [$-2^{\wedge 5}$, $2^{\wedge 5}$], respectively, have been specified in the original KELM. The first parameter C can better off the minimization of fitting errors and the complexity of the model, the second parameter, γ, determines the nonlinear projection from the input area to a large space, and these two key parameters are particularly important to build the classification ability of KELM adapted to the current data set. In order to avoid the uncertainty in experiments caused by large data, before classification, data has been scaled to the range [-1, 1].

Notice that MATLAB simulation experiments were conducted on Windows Server 2018 R2 operator machine, the Xeon CPU E5-2660 v3 (2.60 GHz), and 16 GB of ram. We have charted our results based on fair comparison instructions and as per other works [85–88]. A 10-fold Cross-Validation (CV) is used to evaluate classification results to provide unbiased and objective results. Furthermore, four standard assessment parameters, including Specificity, Sensitivity, classification accuracy (ACC), and Matthews correlation coefficient are included (MCC), have been used for assessing the performance of ECPA-KELM. The detailed definition of the formula can refer to Ref. [89].

6. Experimental findings and analyses

6.1. Results of benchmark functions

6.1.1. The impact of GWO and MFO

In this part, to estimate the effect of diverse mechanisms in ECPA and gain the best strategy combination, we experimented on IEEE CEC2017 30D benchmark tests [90], in this test, each algorithm will be executed 30 times independently. In the algorithms, ECPA means both GWO and MFO are embedded in original CPA, GCPA indicates only GWO is introduced to basic CPA, MCPA shows only MFO is embedded into fundamental CPA. The results of Friedman's test on 30 functions are exhibited in Table 4. From this table, it can be found that ECPA gains the lowest mean level value, 1.25235, and is the best; it signifies the combination between GWO and MFO outperforms single operator GWO or MFO, so the ECPA selected in the subsequent experiment.

6.1.2. Analysis the results of ECPA compared to other algorithms

The benchmark of IEEE CEC2017 was used in this part to measure the property of the ECPA, and in several projects, these benchmarks

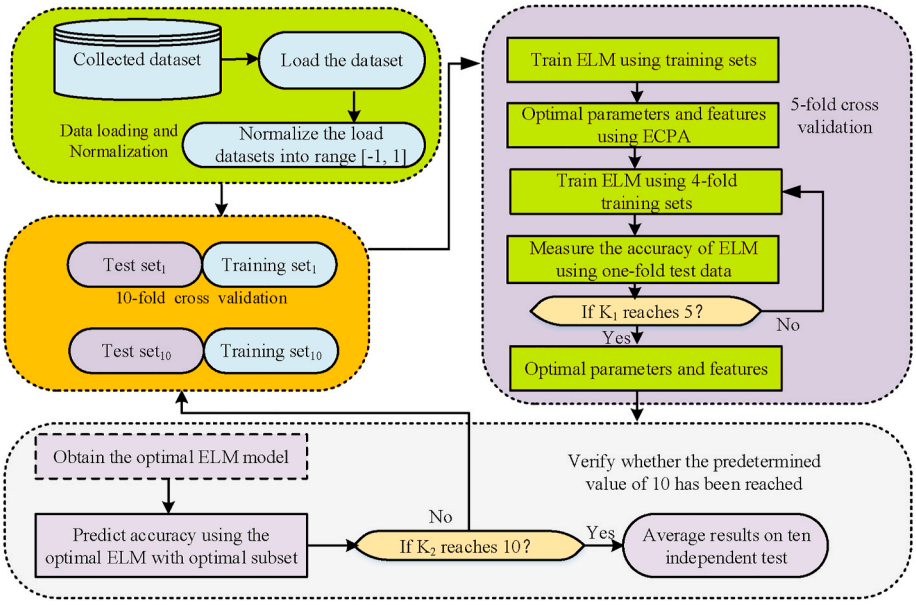

Fig. 1. The Flowchart of the proposed ECPA-KELM.

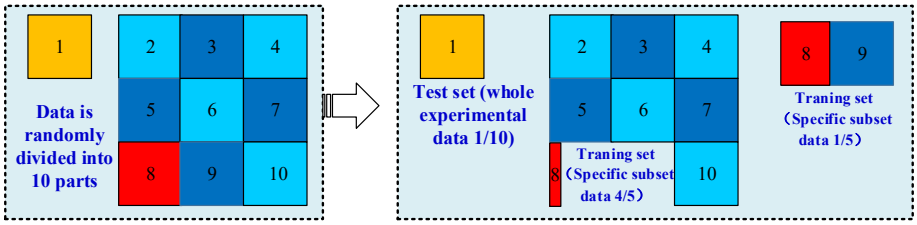

Fig. 2. Data segmentation diagram.

have always been used [90,91]. Furthermore, 30 separate experiments were carried out to mitigate the impact of random variables. In this analysis, the ECPA presented is contrasted with the CPA, CLPSO, DE, PSO, MFO, and GWO algorithms. Thirty individual executions carried out all these approaches to the CEC2017 standards.

In Table 5, the average and standard deviation of the STD is shown to demonstrate detailed experimental results. The average ECPA results shown are the lowest among the benchmarks. Table 6 presents Friedman's ECPA test results against all other rivals. Following the average ranking of the algorithms concerned, the first best results of these benchmarks are disclosed in the ECPA, the worst findings being CPA, CLPSO, DE, PSO, MFO, and GWO. The main features of the current movement techniques abstracted from the grey wolf optimizer and moth-flame optimizer may be a reason for this. In this study, it can be obtained the original CPA between exploration and mining in this analysis.

The convergence curves of these involved algorithms on CEC2017 benchmarks to verify the performance of the designed ECPA are listed in Fig. 3. It can be observed from this figure that the designed ECPA shows the fast conference capabilities and obvious superiority to all other rivals in these CEC 2017 benchmarks. In addition, it also is noted that the designed ECPA has fast convergence searches such as F4, F7, and F9, which guarantee it to quickly obtain a theoretical optimal value. Furthermore, in terms of other benchmarks, the same convergence pattern is also observed. In short, the processes involved can be inferred that the property of the original CPA can significantly enhance.

6.2. Application in the diagnosis of COVID-19 from the perspective of biochemical indicators

In this part, the proposed algorithm ECPA-KELM for diagnosing COVID-19 from the perspective of biochemical indicators is evaluated deeply. Table 7 shows the detailed results of ECPA-KELM on the collected COVID-19 data set. The 92.129% classification accuracy of the ECPA-KELM can be seen from this Table 7, 90.506% of Matthew correlation coefficient, 92.298% of sensitivity, 89.627% of specificity, and their variance is 0.04379, 0.04379, 0.05322, and 0.06536 respectively. Furthermore, we can observe that the proposed ECPA-KELM can automatically acquire the optimum KELM model settings, mainly due to the enhanced ECPA, which can efficiently identify optimum settings and functions.

In addition, the methodology proposed ECPA-KELM is compared to original KELM and other evolutionary computing-based KELM, including CPA-KELM, original KELM, GWO-KELM, MFO-KELM, PSO-KELM, and two common algorithms, SVM and KNN, to check further the property of the ECPA-KELM model presented. Comparisons with accuracy, Matthew coefficient for correlation, susceptibility, specificity, and standard deviation are reported in a detailed statistical experiment in Table 8 and the comparative histogram of each experiment is also shown in Fig. 4 in order to more visually represent the immediate difference in values.

The findings show that the ECPA-KELM algorithm is superior to other competitors and its corresponding standard deviation between all models is also less critical in four evaluation methods such as ACC, MCC, sensitivity, and specificity. In comparison to the original CPA-based KELM, the ECPA-KELM is more efficient and stable obviously. It should be noted that the original KELM, original SVM and KNN are all

Table 3
Benchmark tests of IEEE CEC2017.

ID	Name of the function	Class	Search Range	Optimum
F1	Shifted and Rotated Bent Cigar Function	Unimodal	[-100, 100]	100
F2	Shifted and Rotated Sum of Different Power Function	Unimodal	[-100, 100]	200
F3	Shifted and Rotated Zakharov Function	Unimodal	[-100, 100]	300
F4	Shifted and Rotated Rosenbrock's Function	Multimodal	[-100, 100]	400
F5	Shifted and Rotated Rastrigin's Function	Multimodal	[-100, 100]	500
F6	Shifted and Rotated Expanded Scaffer's F6 Function	Multimodal	[-100, 100]	600
F7	Shifted and Rotated Lunacek Bi-Rastrigin Function	Multimodal	[-100, 100]	700
F8	Shifted and Rotated Non-Continuous Rastrigin's Function	Multimodal	[-100, 100]	800
F9	Shifted and Rotated Lévy Function	Multimodal	[-100, 100]	900
F10	Shifted and Rotated Schwefel's Function	Multimodal	[-100, 100]	1000
F11	Hybrid Function 1 (N=3)	Hybrid	[-100, 100]	1100
F12	Hybrid Function 2 (N=3)	Hybrid	[-100, 100]	1200
F13	Hybrid Function 3 (N=3)	Hybrid	[-100, 100]	1300
F14	Hybrid Function 4 (N=4)	Hybrid	[-100, 100]	1400
F15	Hybrid Function 5 (N=4)	Hybrid	[-100, 100]	1500
F16	Hybrid Function 6 (N=4)	Hybrid	[-100, 100]	1600
F17	Hybrid Function 6 (N=5)	Hybrid	[-100, 100]	1700
F18	Hybrid Function 6 (N=5)	Hybrid	[-100, 100]	1800
F19	Hybrid Function 6 (N=5)	Hybrid	[-100, 100]	1900
F20	Hybrid Function 6 (N=6)	Hybrid	[-100, 100]	2000
F21	Composition Function 1 (N=3)	Composition	[-100, 100]	2100
F22	Composition Function 2 (N=3)	Composition	[-100, 100]	2200
F23	Composition Function 3 (N=4)	Composition	[-100, 100]	2300
F24	Composition Function 4 (N=4)	Composition	[-100, 100]	2400
F25	Composition Function 5 (N=5)	Composition	[-100, 100]	2500
F26	Composition Function 6 (N=5)	Composition	[-100, 100]	2600
F27	Composition Function 7 (N=6)	Composition	[-100, 100]	2700
F28	Composition Function 8 (N=6)	Composition	[-100, 100]	2800
F29	Composition Function 9 (N=3)	Composition	[-100, 100]	2900
F30	Composition Function 10 (N=3)	Composition	[-100, 100]	3000

Table 4
The results of Friedman's test for gaining the best strategy combination.

Algorithm	ECPA	GCPA	MCPA	CPA
mean level	1.25235	3.65248	4.68547	5.68547

showing the worst performance for diagnosis of COVID-19 from the perspective of biochemical indicators, which can be preliminarily shown that KELM model selection capacity can be substantially improved by the algorithm proposed ECPA in this article and the ability to solve the accurate diagnosis of COVID-19 from the perspective of biochemical indicators. The second output of the KELM-based GWO-KELM is just under the ECPA-KELM, and the MFO-KELM and PSO-KELM perform very similar properties on this collected data. In this experiment, we can see that ECPA-KELM can automatically get the best property among all of these competing models, mostly because of the improved ECPA, where the optimal KELM parameters and the optimal subset of functions can be found automatically.

Furthermore, the designed ECPA is used to perform parameter optimization and feature selection simultaneously for KELM to diagnose COVID-19 from the perspective of biochemical indicators. In this analysis, during the feature selection, the 10-fold CV method is used. The detailed selected amount of individual features and statistical values in each 10-fold cycle is shown in Table 9. It can be observed that the ECPA-KELM proposed clearly exceeds others, and regarding the statistics, the features AGE, ALT, ALB, A/G, AST, and LDH were selected with values 9, 8, 9, 8, 9, and 8 respectively by the ECPA-KELM, while The other features have been comparatively picked with less. However, these features were not met by other rivals. Consequently, it can be inferred that such features, which often seem to be present, early recognition of COVID-19 and discrimination of other low-frequency features. Accordingly, due to the underlying details in these frequency features, further consideration should be provided in practice medical cases for these features of AGE, ALT, ALB, A/G, AST, and LDH.

In addition, the comparison results among these methods in terms of CPU time via 10-fold CV is recorded in Fig. 5. It can be observed that the original KELM consumes the least time and its execution speed is the fastest among all these algorithms, the original SVM takes the second least time. An explainable reason is that without the assistance of search algorithms, it will save a lot of algorithm execution time compared to those models-based search algorithms and the incidental result is that the classification performance of the algorithm is greatly reduced. It can also be noted that the designed ECPA-KELM consumes only the fourth-least time, which is more time than the original CPA-KELM, and it shows that the addition operator does increase the execution time of the algorithm. It is also worth noting that the time consumed by KNN and GWO-KELM to deal with this problem is close to the same and among all the algorithms, this PSO-KELM consumes the most time on this problem. A preliminary conclusion can be drawn that although the ECPA-KELM is not the least in terms of CPU consumption time, the four measurement values of it are the best, which also points us to a future research direction through reasonable parallel programming technique to achieve the reduction of CPU consumption time for ECPA-KELM.

7. Discussion

In the present study, the diagnosis of COVID-19 from the perspective of biochemical indicators was investigated by using ECPA to perform KELM optimization parameters and feature selection simultaneously. Importantly, several key features were discovered, the features of AGE, ALT, ALB, A/G, AST, and LDH. Subsequently, an ECPA-KELM model is designed from the perspective of biochemical markers for an effective diagnosis of COVID-19. Thus, we think that the ECPA - KELM model will help to inform the decision-making process.

According to our observations, the proposed CPA-based method has shown enhanced exploratory and exploitative patterns to deal with more complex spaces can also, such as evaluation of human lower limb motions [92], Lunar impact crater identification and age estimation [93], shape registration [94], regression tasks [95], 3D deformable shape analysis [96,97], active surveillance [98], service ecosystem [99,100], and micro-expression spotting [101,102]. Also, we can test explorative features base on more classes of problems such as image editing [103–105], engineering optimization problems [106,107], brain function prediction [108], epidemic prevention and control [109,110], large scale network analysis [111], energy storage planning and scheduling [112], image dehazing [113–115], social recommendation and

Table 5
The statistical experiment results and the comparison algorithms on the test benchmarks.

Algorithm	F1		F2		F3		F4		F5	
	mean	STD	mean	STD	mean	STD	mean	STD	mean	STD
ECPA	**7519.710679**	**8874.468337**	**2.04221E+90**	**9.13306E+90**	314838.9408	170596.2497	**687.3605381**	**49.76192334**	**1088.571685**	**43.01335698**
CPA	58067616.71	34335129.37	5.6031E+109	2.4825E+110	283553.8801	22234.31676	951.0959434	63.02705513	1256.720481	196.764764
CLPSO	1.83393E+11	24500918385	6.1024E+169	65535	700559.2882	47420.25288	50903.24199	7796.56118	2175.886699	82.37715166
DE	215908522.4	142952364.7	3.3748E+152	1.0077E+153	**285471.1581**	**59737.93336**	1025.661518	103.2197059	1580.943344	21.75055725
PSO	1991512282	127980323.2	8.68129E+84	1.8012E+85	366925.2549	57606.63467	976.4864367	79.9830326	1727.534556	72.72507397
MFO	1.26938E+11	33282042998	4.3664E+159	65535	961441.4082	176082.2006	27266.83621	13634.84439	1788.753042	170.7635689
GWO	45349270909	9389026366	3.4903E+134	1.5609E+135	391307.7296	40785.9763	4664.67888	1005.825016	1190.601048	116.2702424
Algorithm	**F6**		**F7**		**F8**		**F9**		**F10**	
	mean	STD	mean	STD	mean	STD	mean	STD	mean	STD
ECPA	**600.6797401**	**0.726360312**	**1557.960993**	**64.86428666**	**1351.760045**	**35.2623542**	**7524.304454**	**4161.825874**	**21697.1674**	**958.8201343**
CPA	601.1526004	0.535879883	1950.036203	53.21684409	1651.676645	148.1956341	23413.93197	3861.054153	28492.71778	806.4821693
CLPSO	704.332919	5.781684018	4709.125525	244.682567	2551.597914	83.83139597	144748.0043	10676.28984	29668.53845	753.6499009
DE	606.5155211	0.548722584	1957.043926	26.25937571	1866.615326	25.28693829	34717.15906	5864.382307	31541.0577	627.1407208
PSO	696.5894893	4.101100271	2025.001303	143.2750109	2149.27231	65.26497146	70208.35689	6631.34449	26763.20186	1775.78292
MFO	678.9754316	8.221739928	5099.252286	743.515249	2105.101929	143.3009662	50290.07664	6053.136405	17871.43667	1586.848038
GWO	637.3324028	4.16929005	2090.056294	185.7821258	1462.43793	67.56033436	42103.97034	9625.579122	16526.22378	1322.128908
Algorithm	**F11**		**F12**		**F13**		**F14**		**F15**	
	mean	STD	mean	STD	mean	STD	mean	STD	mean	STD
ECPA	**18953.19336**	**25854.43115**	**2693789.161**	**1383552.068**	**6589.122975**	**5884.094007**	**228633.6083**	**673489.9711**	**4031.694125**	**2313.713192**
CPA	19830.37394	4996.263472	52227549.9	17330520.18	6676.660636	3588.867665	976879.7906	416109.6933	2985.822586	1173.253232
CLPSO	284007.5699	46750.90608	87406551875	11616002337	15952751134	3856348973	106691154.6	41839869.01	6611655778	1422797557
DE	185284.6424	29258.83368	2408635693	327025998.7	386948.2598	744213.7998	31784999.58	7263830.515	804272.1577	795228.7315
PSO	9664.308497	1346.604875	1503616186	351060611.9	114504727	9766687.809	3688485.076	1022032.508	44607692.95	7679413.445
MFO	221722.4462	104031.3324	33545947708	13372135809	5920423082	4514262522	17247809.91	16515861.39	1205521179	1040612230
GWO	70261.36301	12967.45317	8844852431	4314498259	1002827330	887848506.6	7093501.761	3457695.4	251397816.4	395962112.3
Algorithm	**F16**		**F17**		**F18**		**F19**		**F20**	
	mean	STD	mean	STD	mean	STD	mean	STD	mean	STD
ECPA	**6532.432694**	**392.8143904**	**5482.224614**	**387.4351012**	**1007519.361**	**2488467.227**	5981.503978	5250.553821	**5814.249303**	**393.2756621**
CPA	7901.830961	756.4821831	5900.118702	386.0372861	1579385.81	666778.6832	6367.962479	1488.584253	6374.135454	363.0730879
CLPSO	15293.95602	871.7305561	310364.4258	423969.8767	109921769.7	36078708.47	5991270333	1824921832	7383.862904	227.260953
DE	11006.33391	333.1618092	7441.137175	242.3668843	68262535.8	17182048.88	**4367.962479**	**7203099.89**	7206.672918	264.1567812
PSO	8805.56367	843.2325756	6640.489183	479.8415523	4935369.623	1452155.002	51561178.86	11690487.47	6378.707086	530.4246744
MFO	8127.247152	996.6102452	9562.367243	6082.259602	20921941.57	19780428.09	1183602970	1812415825	5976.81213	646.0137233
GWO	6574.513125	810.9509249	5065.658247	473.4615271	8635621.082	5514476.287	177360649.9	284908174.6	5607.906089	1212.15523
Algorithm	**F21**		**F22**		**F23**		**F24**		**F25**	
	mean	STD	mean	STD	mean	STD	mean	STD	mean	STD
ECPA	**2890.433021**	**41.63147492**	24439.47999	983.9609558	**3315.175463**	**38.15305085**	**3842.473323**	**63.55602103**	**3322.94086**	**57.33105562**
CPA	3017.135124	228.4465442	31255.1438	646.2200858	3588.721134	123.1973624	3788.375225	178.0840806	3655.90184	81.07503213
CLPSO	4242.074914	98.27685524	31847.07587	1390.221732	5295.468269	177.5978616	7323.635137	402.5075032	28115.05342	3426.961738
DE	3412.116102	23.29958151	33541.21457	551.4043055	3731.382815	22.14700112	4259.720459	37.1922972	4230.851635	81.12705677
PSO	3952.566818	162.3811005	29742.15427	1036.080537	5203.998987	332.7917067	6408.489575	408.3690984	3581.99979	62.96151877
MFO	3680.993214	130.4138229	**20943.98947**	**2140.785308**	3832.470907	99.09279821	4403.179372	153.4534976	13589.26927	5650.487238
GWO	2999.920857	146.5631493	20195.99366	1501.497233	3621.578759	73.51777033	4263.283846	160.4600932	6707.051128	853.1706782
Algorithm	**F26**		**F27**		**F28**		**F29**		**F30**	
	mean	STD	mean	STD	mean	STD	mean	STD	mean	STD
ECPA	**11606.49623**	**446.9301218**	**3549.623042**	**65.25445033**	**3434.416563**	**34.09136414**	**6883.147807**	**336.6599858**	**10742.77366**	**6152.189641**
CPA	13206.99244	1371.738498	3859.000673	98.80544307	3968.084533	96.77582415	7910.657826	674.6082742	165589.0055	90086.83137
CLPSO	40704.31025	2745.864995	7645.650413	665.0340232	32600.64241	1741.460858	82911.56839	54047.75509	11856029494	4049036860
DE	16308.07735	296.64459	4083.747208	97.22886489	4781.849118	567.3122875	9547.829534	348.1264729	2444619.988	791171.508
PSO	21960.11019	6292.488945	3464.714421	292.1733505	3568.921159	50.62671127	10913.7073	929.817046	251016748.8	106953202.2
MFO	18343.68491	1357.92059	4135.749521	377.4549831	19469.60896	1812.532639	30933.00976	82123.3563	2884115452	2206795617
GWO	15387.13244	1092.682552	4103.883125	173.0776863	9034.098479	1213.571325	8656.925738	1023.439226	1121182797	843139483.4

Table 6
The results of Friedman's test over these involved algorithms.

Algorithm	ECPA	CPA	CLPSO	DE	PSO	MFO	GWO
mean level	1.35685	6.523696	3.6322222	3.65214	4.254141	4.012544	3.5624156

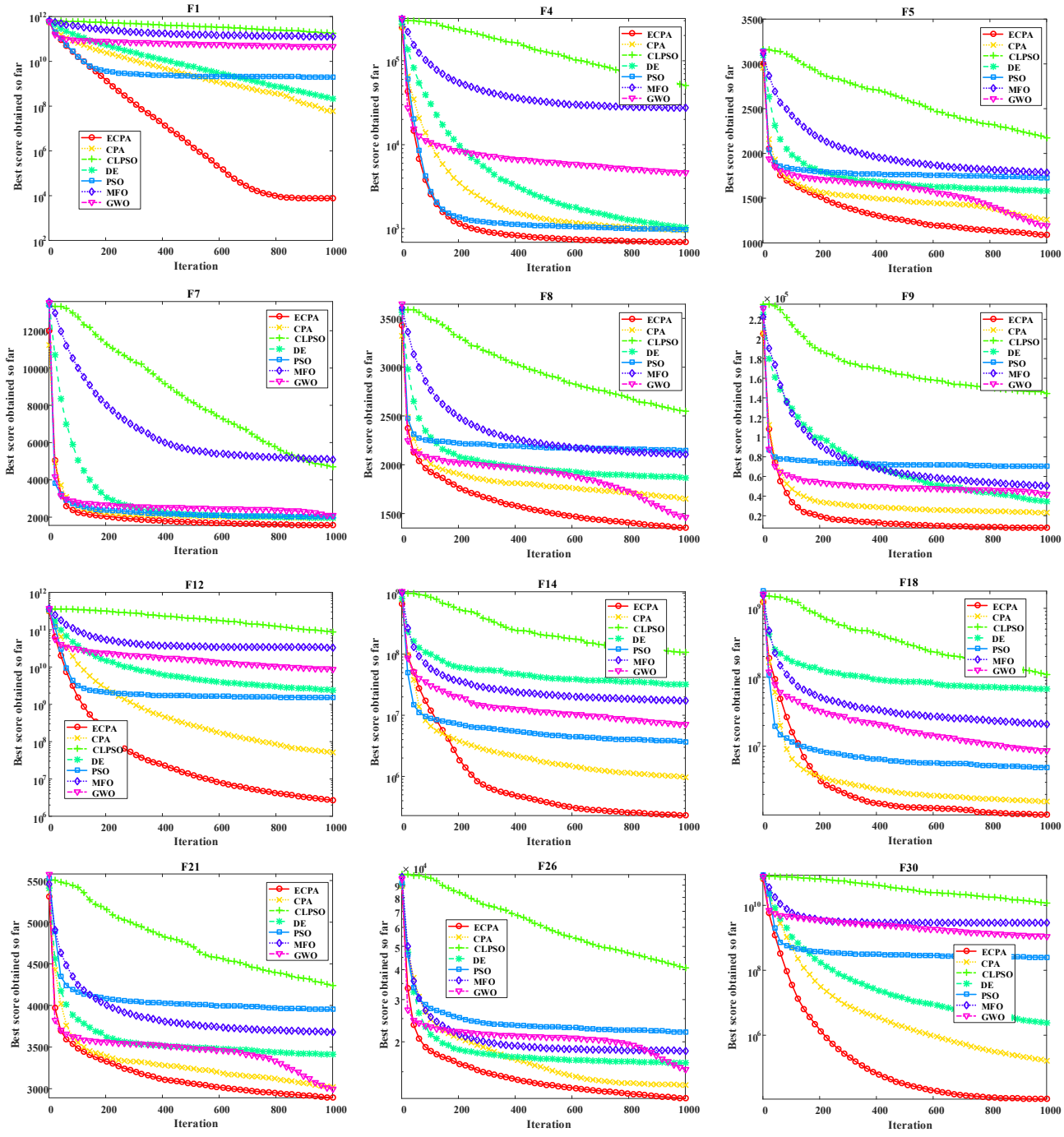

Fig. 3. Convergence curves of selected benchmark functions.

QOS-aware service composition [116–118], medical diagnosis [119–122], covert communication system [123, 124], pedestrian dead reckoning [125], and feature selection [126–128].

Several studies have shown that age is one of the main risks of respiratory system diseases [129,130]. In terms of SARS and MERS, older age was an independent predictor of SARS or MERS exacerbation risk and mortality [131–133]. Similarly, a large body of studies confirms that advanced age patients are more susceptible to COVID-19 infections than young patients and older age patients are more susceptible to severe COVID-19 [134,135]. Meanwhile, researchers have also shown that age is an independent pronouncing factor for COVID-19 [134,136]. There are several possible reasons to explain this phenomenon. First, immune-senescence in aging is considered to be the leading cause of severe pneumonia mortality in older adults [129]. Second, with the

Table 7
The results of ECPA-KELM on collected data.

Fold	ACC	MCC	Sensitivity	Specificity
#1	0.8859	0.8656	0.9695	0.82
#2	0.8932	0.8863	0.8956	0.8632
#3	0.9623	0.9575	0.9625	0.8852
#4	0.9773	0.8425	0.8857	0.8958
#5	0.9763	0.8895	0.9659	0.9623
#6	0.8968	0.9462	0.8352	0.9528
#7	0.8867	0.8754	0.9584	0.9782
#8	0.9732	0.8989	0.8758	0.8025
#9	0.8897	0.9325	0.9953	0.8369
#10	0.8778	0.9562	0.8859	0.9658
Mean	**0.92192**	**0.90506**	**0.92298**	**0.89627**
STD	**0.04379**	**0.04054**	**0.05322**	**0.06536**

increase of age, the cellular and humoral immune function of the body gradually declines [137–139]. For example, the level of immunoglobulin M and interferon decrease, the number of T- and B-lymphocyte decreases, resulting in an increased risk of infection [140]. Third, older COVID-19 patients tended to have more commodities, which was easier to acute respiratory failure and have a poor prognosis [141,142]. Similar to their results, we found that the extreme COVID-19 group's mean age was 1.45 times higher than that of a non-severe COVID-19 group ($P = 0.00$), indicating that age could be considered a promising clinical outcome index in COVID-19 patients.

It was notified that approximately 60% of SARS patients have liver impairment [143]. Likewise, MERS patients also have liver damage [144]. Numerous retrospective studies have demonstrated that COVID-19 patients often have liver function damage. Based on the large retrospective data, increased levels of ALT and AST have been found in 14–53% of patients with COVID-19 [145,146]. The most widely used parameters are ALT and AST liver functions. The permeability of the cell membrane will increase if hepatocytes are affected. The blood circulation is freed by high levels of cytoplasmic transaminases such as alanine aminotransferase, aspartate aminotransferase, and complete bilirubin [147,148]. Many studies confirm that in extreme COVID-19 patients, ALT and AST were substantially higher than in non-severe patients [149]. However, the mechanism of SARS-CoV-2-induced liver impairment is not as yet clear. First, the cytokine storm following SARS-CoV-2 infection is thought to be one of the key factors of liver impairment [150]. Second, SARS-CoV-2 may directly be infecting hepatocytes. Xu and colleagues confirmed that the main pathologies of the liver in COVID-19 patients were characterized by moderate microvascular steatosis, mild lobular and portal activity [150]. In this analysis, we also found, relative to the non-extreme COVID-19 group, that the levels of ALT and AST in the severe COVID-19 group were 2.73 and 2.83 times higher. In summary, the association between liver function damage and COVID-19, a major factor in COVID-19 progression closely linked to COVID-19 seriousness, was revealed in these results.

Another important biomarker, albumin (ALB), is one of the indexes of liver impairment [151]. ALB is synthesized by parenchymal cells in the liver, and the plasma half-life of albumin in the plasm is 15–19 days [152]. The level of ALB reflects the synthetic protein function of the liver, and ALB is a useful index for assessing nutritional status. He et al. found that plasma ALB levels are positively associated with the degree of community-acquired pneumonia (CAP) in pregnancy [153]. Recently, future analysis of over 400 CAP patients found a substantially higher

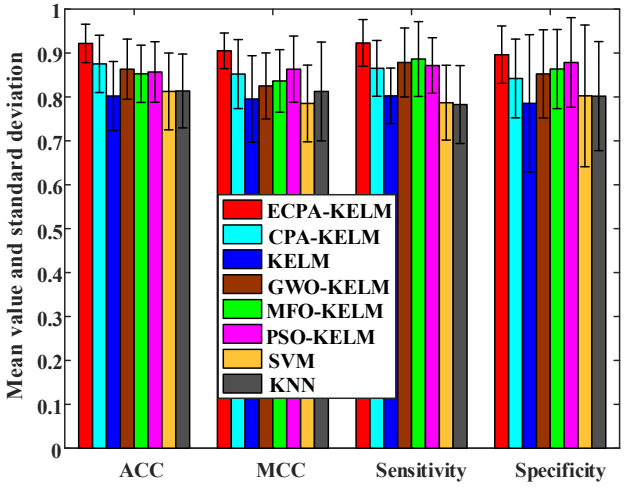

Fig. 4. The comparison in terms of the four metrics and standard deviation.

Table 9
The numbers of selected feature.

Index	Algorithms				
	ECPA-KELM	CPA-KELM	GWO-KELM	MFO-KELM	PSO-KELM
F1	0	0	0	1	2
F2	9	7	8	8	7
F3	3	3	4	5	5
F4	4	5	3	3	5
F5	8	7	8	7	7
F6	2	4	5	5	4
F7	9	7	6	6	7
F8	2	3	4	5	4
F9	8	8	7	6	6
F10	5	4	4	6	4
F11	3	5	5	6	4
F12	9	8	7	7	8
F13	1	2	4	4	5
F14	8	7	7	6	6
F15	4	5	3	5	4
F16	6	5	2	4	3
F17	4	5	5	3	4
F18	2	5	5	3	6
F19	1	6	4	6	4
F20	4	5	4	5	3
F21	3	5	5	3	3
F22	2	4	6	4	4
F23	1	6	5	1	1
F24	2	4	4	2	6
F25	6	6	6	5	5

Table 8
The statistical experiment results of comparison in terms of the four metrics.

Algorithms	ACC	MCC	Sensitivity	Specificity
ECPA-KELM	**0.92192 ± 0.04379**	**0.90506 ± 0.04054**	**0.92298 ± 0.05322**	**0.89627 ± 0.06536**
CPA-KELM	0.87523 ± 0.06521	0.85214 ± 0.07854	0.86521 ± 0.06352	0.84215 ± 0.08965
KELM	0.80215 ± 0.07851	0.79541 ± 0.09851	0.80251 ± 0.06325	0.78541 ± 0.15632
GWO-KELM	0.86325 ± 0.06852	0.8251 ± 0.07513	0.87854 ± 0.07852	0.85247 ± 0.10043
MFO-KELM	0.85264 ± 0.06528	0.83652 ± 0.0712	0.88635 ± 0.08521	0.86354 ± 0.09013
PSO-KELM	0.85684 ± 0.06892	0.86325 ± 0.0754	0.87169 ± 0.06323	0.87854 ± 0.10212
SVM	0.81256 ± 0.08751	0.78521 ± 0.0874	0.78693 ± 0.08521	0.80254 ± 0.16134
KNN	0.81365 ± 0.08411	0.81254 ± 0.1125	0.78265 ± 0.08874	0.8019 ± 0.12415

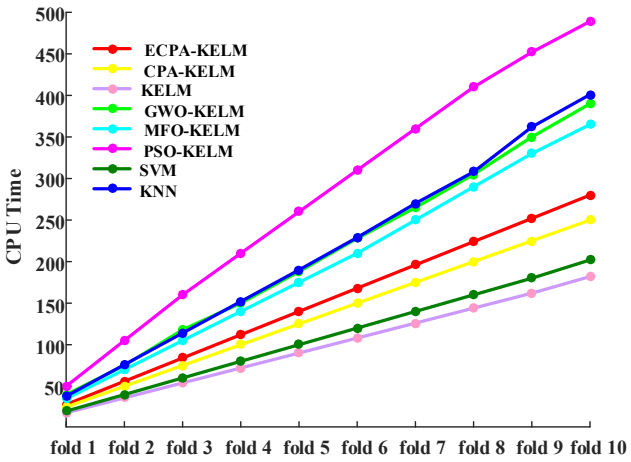

Fig. 5. Comparison results among these methods in terms of CPU time via 10-fold CV.

plasma ALB level in the community of survivors than in the non-survivor group, indicating that ALB could be promising for CAP pronostics [154]. In line with these findings, Liu et al. found that plasma ALB levels in the group COVID-19 were considerably lower than in the group COVID-19 stabilization (36.62 ± 6.60 g/L vs. 41.27 ± 4.55 g/L), suggesting hypoalbuminemia was positively associated with advanced COVID-19 progression and ALB may be used as an independent predictor of severity of illness and outcome [155,156]. Consistent with their findings, in the current study, we also revealed that plasma ALB levels in the severe COVID-19 group were significantly lower than the non-severe COVID-19 group (35.90 ± 4.65 vs. 41.53 ± 2.57, P = 0.000). In addition, globulin is the main component of serum non-albumin protein, which is composed of various pro-inflammatory proteins, such as immunoglobulin, complement, and C-reactive protein. Serum globulin levels are an objective marker to reflect the systemic inflammation and the immune status of the body [157,158]. Of note, in recent years, Albumin/Globulin ratio (A/G) was commonly used to detect infectious diseases such as the acute exacerbation of the chronic obstructive pulmonary disease, hepatitis C and human immunodeficiency virus infection as a quick and inexpensive biomarker [159–161]. Furthermore, A/G also can be used as a novel predictor of prognosis in patients with a malignant tumor, including hepatocellular carcinoma, laryngeal squamous cell carcinoma, and colorectal cancer [162,162]. However, few studies have reported on the relationship between A/G and COVID-19 patients. Universal research used by Zhou et *al.* shows that A/G was substantially related to COVID-19 severity. However, as shown by the multivariate binary logistic regression model, A/G was not an independent risk element for patients with COVID-19 [4]. Our analysis showed that in non-serious COVID-19 groups, A/G was substantially higher with approximately 1,41 times the amount of extreme COVID-19 groups (1.68 ± 0.24 vs. 1.19 ± 0.36, P = 0.000). This is the first time we realize that machine learning is being used to incorporate the A/G variable into COVID-19 research. All in all, the plasma ALB levels and The value for discrimination against COVID-19 patients A/G were shown to be significantly predictive and might predict COVID-19 progression.

Lactate dehydrogenase (LDH) is an essential energy-producing enzyme required for human physiology. LDH is present in almost all tissues, including liver, lung, kidney, skeletal muscle, myocardium tissue. Many studies have shown that elevated LDH levels are associated with disease progression and poor clinical outcome [163,164]. For instance, a population-based study of 238 cases of SARS from Singapore suggested that high LDH is positive for adverse outcomes and acute syndrome of air distress [165]. Chang and colleagues reported that elevated LDH levels were related to increased mortality in SARS cases [166]. Therefore, LDH is a potential risk prediction factor. Recent seven studies, including a meta-analysis with >1900 COVID-19 patients, found that the increased LDH level has been substantially linked to COVID-19 severity [167]. Our study found that the average LDH of the severe COVID-19 group was 382.95 ± 152.78, and that of the non-severe COVID-19 group was 244.37 ± 61.07, suggesting that plasma LDH levels may be regarded as a promising biomarker of clinical outcome in COVID-19 patients.

So far, very few relevant studies describing biochemical index, blood electrolyte, and clinical parameters to joint predict the severity and prognosis of the COVID-19. This is the first effort to incorporate age, ALT, AST, ALB, A/G, and LDH for predicting and discriminating COVID-19 severity using the machine learning method. However, some limitations exist in our research. First, the number of COVID-19 cases was relatively small, and patient data came from a single center. The model constructed ECPA-KELM can provide early warning for the severity of COVID-19 and help clinicians in the diagnosis and treatment of this infectious disease. In the future, we hope to enlarge the sample size and to improve the accuracy of the ECPA-KELM model further. Second, independent/external datasets or prospective studies are needed to verify the accuracy of the ECPA-KELM model to make the model more reliable and stable.

8. Conclusion and future work

The study uses clinical information from the Affiliated Yuqing Hospital of the Medical University of Wenzhou to develop an efficient ECPA-KELM early identification procedure and COVID-19 discrimination (Yueqing, China). The main innovation for the proposed methodology is for the current ECPA to include a new strategy to enhance and restore the original CPA search ability; the performance of the ECPA has been strictly regulated with the CEC2017 criteria compared with several other rivals. Experimental findings indicate that the ECPA proposed is much better suited than others to achieve this function optimization. In addition, ECPA has been proposed for the synchronized evolution of the optimum parameters and feature selection in KELM; the resulting ECPA-KELM was used successfully for early identification and discrimination against COVID-19. There has also been a rigorous analysis of the ECPA-KELM with other competitive algorithms. The findings also showed that the ECPA-KELM predicts the more stable properties more accurately and can be treated as a tool to provide early warning for the severity of COVID-19 and help clinicians in the diagnosis and treatment of this infectious disease.

For future work, a number of matters can be further investigated. More variables and coefficients are added, and parallel processing can also reduce the computing burden in the application phase; the following should be noted. We can also increase the number of data samples to create a safer and more effective prediction system. In addition, the proposed ECPA-KELM can also be employed to predict other variety of conditions such as clustering aspects and splitting the used image into CTs to expand the use of the developed system.

Acknowledgments

Beibei Shi and Hua Ye contributed equally to this paper and are co-first authors. Huiling Chen, and Peiliang Wu also contributed equally to this work and are co-corresponding authors. This research was supported by the Key Project of Zhejiang Provincial Natural Science Foundation under Grant (LD21F020001) and the National Natural Science Foundation of China (62076185, U1809209).

References

[1] Qun Li, Xuhua Guan, Peng Wu, Xiaoye Wang, Lei Zhou, Yeqing Tong, Ruiqi Ren, Kathy SM. Leung, H.Y. Eric, Lau, Jessica Y. Wong, et al., Early transmission dynamics in wuhan, China, of novel coronavirus–infected pneumonia, N. Engl. J. Med. 382 (2020) 1199–1207.

[2] Dilbag Singh, Vijay Kumar, Manjit Kaur, et al., Classification of covid-19 patients from chest ct images using multi-objective differential evolution–based convolutional neural networks, Eur. J. Clin. Microbiol. Infect. Dis. 39 (7) (2020) 1379–1389.

[3] Aleksandra Klimczak, Perspectives on mesenchymal stem/progenitor cells and their derivates as potential therapies for lung damage caused by covid-19, World J. Stem Cell. 12 (9) (2020) 1013.

[4] Xiaohui Liu, Si Shi, Jinling Xiao, Hongwei Wang, Liyan Chen, Jianing Li, Kaiyu Han, Prediction of the severity of corona virus disease 2019 and its adverse clinical outcomes, Japanese journal of infectious diseases 73 (6) (2020) 404–410.

[5] Yafei Zhang, Xiaodan Zhang, Lan Liu, Hongling Wang, Qiu Zhao, Suggestions for infection prevention and control in digestive endoscopy during current 2019-ncov pneumonia outbreak in wuhan, hubei province, China, Endoscopy 52 (4) (2020) 312.

[6] Mingwu Zhang, Yu Chen, Willy Susilo, Ppo-cpq: a privacy-preserving optimization of clinical pathway query for e-healthcare systems, IEEE Internet of Things Journal 7 (10) (2020) 10660–10672.

[7] Hwang De-Kuang, Hsu Chih-Chien, Chang Kao-Jung, Chao Daniel, Sun Chuan-Hu, Jheng Ying-Chun, A. Aliaksandr, Yarmishyn, Wu Jau-Ching, Tsai Ching-Yao, Wang Mong-Lien, et al., Artificial intelligence-based decision-making for age-related macular degeneration, Theranostics 9 (1) (2019) 232.

[8] Minhaj Alam, David Le, Jennifer I. Lim, Robison VP. Chan, Xincheng Yao, Supervised machine learning based multi-task artificial intelligence classification of retinopathies, J. Clin. Med. 8 (6) (2019) 872.

[9] Qinghua Jiang, Guohua Wang, Shuilin Jin, Yu Li, Yadong Wang, Predicting human microrna-disease associations based on support vector machine, Int. J. Data Min. Bioinf. 8 (3) (2013) 282–293.

[10] Pingli Dong, Tingting Zhang, Huijing Xiang, Xue Xu, Yihui Lv, Yi Wang, Chichong Lu, Controllable synthesis of exceptionally small-sized superparamagnetic magnetite nanoparticles for ultrasensitive mr imaging and angiography, J. Mater. Chem. B 9 (4) (2021) 958–968.

[11] Zhijie Wang, Tingting Zhang, Lei Pi, Huijing Xiang, Pingli Dong, Chichong Lu, Tian Jin, Large-scale one-pot synthesis of water-soluble and biocompatible upconversion nanoparticles for dual-modal imaging. Colloids and Surfaces B: Biointerfaces 198 (2021) 111480.

[12] Daniel S. Kermany, Michael Goldbaum, Wenjia Cai, Carolina CS. Valentim, Huiying Liang, Sally L. Baxter, Alex McKeown, Ge Yang, Wu Xiaokang, Yan Fangbing, et al., Identifying medical diagnoses and treatable diseases by image-based deep learning, Cell 172 (5) (2018) 1122–1131.

[13] Lei Wang, Shujian Yang, Shan Yang, Cheng Zhao, Guangye Tian, Yuxiu Gao, Yongjian Chen, Yun Lu, Automatic thyroid nodule recognition and diagnosis in ultrasound imaging with the yolov2 neural network, World J. Surg. Oncol. 17 (1) (2019) 1–9.

[14] Ziad Obermeyer and Ezekiel J Emanuel, Predicting the future—big data, machine learning, and clinical medicine, N. Engl. J. Med. 375 (13) (2016) 1216.

[15] Sheshadri Iyengar Raghavan Bhagyashree, Kiran Nagaraj, Martin Prince, Caroline HD Fall, Murali Krishna, Diagnosis of dementia by machine learning methods in epidemiological studies: a pilot exploratory study from south India, Soc. Psychiatr. Psychiatr. Epidemiol. 53 (1) (2018) 77–86.

[16] Soo-Kyoung Lee, Youn-Jung Son, Jeongeun Kim, Hong-Gee Kim, Jae-Il Lee, Bo-Yeong Kang, Hyeon-Sung Cho, Sungin Lee, Prediction model for health-related quality of life of elderly with chronic diseases using machine learning techniques, Healthcare informatics research 20 (2) (2014) 125.

[17] Kaiyang Qu, Leyi Wei, Quan Zou, A review of dna-binding proteins prediction methods, Curr. Bioinf. 14 (3) (2019) 246–254.

[18] A.S. Albahri, Rula A. Hamid, Jwan K. Alwan, Z.T. Al-Qays, A.A. Zaidan, B. B. Zaidan, A.O.S. Albahri, A.H. AlAmoodi, Jamal Mawlood Khlaf, E.M. Almahdi, et al., Role of biological data mining and machine learning techniques in detecting and diagnosing the novel coronavirus (covid-19): a systematic review, J. Med. Syst. 44 (2020) 1–11.

[19] Hengyuan Kang, Liming Xia, Fuhua Yan, Zhibin Wan, Feng Shi, Huan Yuan, Huiting Jiang, Dijia Wu, He Sui, Changqing Zhang, et al., Diagnosis of coronavirus disease 2019 (covid-19) with structured latent multi-view representation learning, IEEE Trans. Med. Imag. 39 (8) (2020) 2606–2614.

[20] Saleh Albahli, A deep neural network to distinguish covid-19 from other chest diseases using x-ray images, Current medical imaging 17 (1) (2021) 109–119.

[21] Zifeng Yang, Zhiqi Zeng, Ke Wang, Sook-San Wong, Wenhua Liang, Mark Zanin, Peng Liu, Xudong Cao, Zhongqiang Gao, Zhitong Mai, et al., Modified seir and ai prediction of the epidemics trend of covid-19 in China under public health interventions, J. Thorac. Dis. 12 (3) (2020) 165.

[22] Nanning Zheng, Shaoyi Du, Jianji Wang, He Zhang, Wenting Cui, Zijian Kang, Tao Yang, Bin Lou, Yuting Chi, Hong Long, et al., Predicting covid-19 in China using hybrid ai model, IEEE transactions on cybernetics 50 (7) (2020) 2891–2904.

[23] Ashkan Ebadi, Pengcheng Xi, Stéphane Tremblay, Bruce Spencer, Raman Pall, Alexander Wong, Understanding the temporal evolution of covid-19 research through machine learning and natural language processing, Scientometrics 126 (1) (2021) 725–739.

[24] Ricardo C. Cury, Istvan Megyeri, Tony Lindsey, Robson Macedo, Juan Batlle, Shwan Kim, Brian Baker, Robert Harris, Reese H. Clark, Natural language processing and machine learning for detection of respiratory illness by chest ct imaging and tracking of covid-19 pandemic in the us, Radiology: Cardiothoracic Imaging 3 (1) (2021) e200596.

[25] Parnian Afshar, Shahin Heidarian, Nastaran Enshaei, Farnoosh Naderkhani, Moezedin Javad Rafiee, Anastasia Oikonomou, Faranak Babaki Fard, Kaveh Samimi, Konstantinos N. Plataniotis, Arash Mohammadi, Covid-ct-md, covid-19 computed tomography scan dataset applicable in machine learning and deep learning, Scientific Data 8 (1) (2021) 1–8.

[26] Muhammad EH. Chowdhury, Tawsifur Rahman, Amith Khandakar, Somaya Al-Madeed, Susu M. Zughaier, Suhail AR. Doi, Hanadi Hassen, Mohammad T. Islam, An early warning tool for predicting mortality risk of covid-19 patients using machine learning, Cognitive Computation (2021) 1–16.

[27] Anuj Tiwari, Arya V. Dadhania, Vijay Avin Balaji Ragunathrao, Edson RA. Oliveira, Using machine learning to develop a novel covid-19 vulnerability index (c19vi), Sci. Total Environ. 773 (2021) 145650.

[28] Guohua Wu, Rammohan Mallipeddi, Ponnuthurai Nagaratnam Suganthan, Problem definitions and evaluation criteria for the cec 2017 competition on constrained real-parameter optimization, National University of Defense Technology, Changsha, Hunan, PR China and Kyungpook National University, Daegu, South Korea and Nanyang Technological University, Singapore, Technical Report (2017).

[29] Jihong Pang, Hongming Zhou, Ya-Chih Tsai, Fuh-Der Chou, A scatter simulated annealing algorithm for the bi-objective scheduling problem for the wet station of semiconductor manufacturing, Comput. Ind. Eng. 123 (2018) 54–66.

[30] Hongming Zhou, Jihong Pang, Ping-Kuo Chen, Fuh-Der Chou, A modified particle swarm optimization algorithm for a batch-processing machine scheduling problem with arbitrary release times and non-identical job sizes, Comput. Ind. Eng. 123 (2018) 67–81.

[31] Dong Zhao, Lei Liu, Fanhua Yu, Ali Asghar Heidari, Mingjing Wang, Diego Oliva, Khan Muhammad, Huiling Chen, Ant colony optimization with horizontal and vertical crossover search: fundamental visions for multi-threshold image segmentation, Expert Syst. Appl. (2020) 114122, https://doi.org/10.1016/j.eswa.2020.114122.

[32] Dong Zhao, Lei Liu, Fanhua Yu, Ali Asghar Heidari, Mingjing Wang, Guoxi Liang, Khan Muhammad, Huiling Chen, Chaotic random spare ant colony optimization for multi-threshold image segmentation of 2d kapur entropy, Knowl. Base Syst. (2020) 106510, https://doi.org/10.1016/j.knosys.2020.106510.

[33] Wu Deng, Hailong Liu, Junjie Xu, Huimin Zhao, Yingjie on Instrumentation Song, and Measurement. An improved quantum-inspired differential evolution algorithm for deep belief network, in: IEEE Transactions On Instrumentation & Measurement, 2020, https://doi.org/10.1109/TIM.2020.2983233.

[34] Huimin Zhao, Haodong Liu, Junjie Xu, Deng Wu, Performance prediction using high-order differential mathematical morphology gradient spectrum entropy and extreme learning machine, IEEE Transactions on Instrumentation & Measurement 69(7) (2019) 4165–4172.

[35] Zhennao Cai, Jianhua Gu, Jie Luo, Qian Zhang, Huiling Chen, Zhifang Pan, Yuping Li, Chengye Li, Evolving an optimal kernel extreme learning machine by using an enhanced grey wolf optimization strategy, Expert Syst. Appl. 138 (2019) 112814.

[36] Caiyang Yu, Mengxiang Chen, Kai Cheng, Xuehua Zhao, Chao Ma, Fangjun Kuang, Huiling Chen, Sgoa: annealing-behaved grasshopper optimizer for global tasks. *Engineering with Computers*, pages 10.1007/s00366–020–01234–1, 2021.

[37] Yanan Zhang, Renjing Liu, Ali Asghar Heidari, Xin Wang, Ying Chen, Mingjing Wang, Huiling Chen, Towards augmented kernel extreme learning models for bankruptcy prediction: algorithmic behavior and comprehensive analysis, Neurocomputing 430 (2020) 185–212.

[38] M. Chen, G. Zeng, K. Lu, J. Weng, A two-layer nonlinear combination method for short-term wind speed prediction based on elm, enn, and lstm, IEEE Internet of Things Journal 6 (4) (2019) 6997–7010.

[39] Abdoul Fatakhou Ba, Hui Huang, Mingjing Wang, Xiaojia Ye, Zhiyang Gu, Huiling Chen, Xueding Cai, Levy-based antlion-inspired optimizers with orthogonal learning scheme, Eng. Comput. (2020) 1–22.

[40] Shubham Gupta, Kusum Deep, Ali Asghar Heidari, Hossein Moayedi, Huiling Chen, Harmonized salp chain-built optimization, Eng. Comput. (2019) 1–31.

[41] Xi Liang, Zhennao Cai, Mingjing Wang, Xuehua Zhao, Huiling Chen, Chengye Li Chaotic, Oppositional sine–cosine method for solving global optimization problems. *Engineering with Computers*, pages 1–17, 2020.

[42] Hongliang Zhang, Zhennao Cai, Xiaojia Ye, Mingjing Wang, Fangjun Kuang, Huiling Chen, Chengye Li, Yuping Li, A multi-strategy enhanced salp swarm algorithm for global optimization. *Engineering with Computers*, pages 1–27, 2020.

[43] Guo-qiang Zeng, Yong-zai Lu, W.J Mao, C Mao. Modified extremal optimization for the hard maximum satisfiability problem, J. Zhejiang Univ. - Sci. C 12 (7) (2011) 589–596.

[44] Guoqiang Zeng, Yongzai Lu, Yuxing Dai, Zhengguang Wu, Weijie Mao, Zhengjiang Zhang, Chongwei, Backbone guided extremal optimization for the hard maximum satisfiability problem, International Journal of Innovative Computing Information and Control 8 (12) (2012) 8355–8366.

[45] Ali Asghar Heidari, Rahim Ali Abbaspour, and Huiling Chen. Efficient boosted grey wolf optimizers for global search and kernel extreme learning machine training, Appl. Soft Comput. 81 (2019) 105521.

[46] Liming Shen, Huiling Chen, Zhe Yu, Wenchang Kang, Bingyu Zhang, Huaizhong Li, Bo Yang, Dayou Liu, Evolving support vector machines using fruit fly optimization for medical data classification, Knowl. Base Syst. 96 (2016) 61–75.

[47] Mingjing Wang, Huiling Chen, Chaotic multi-swarm whale optimizer boosted support vector machine for medical diagnosis, Appl. Soft Comput. 88 (2020) 105946.

[48] Mingjing Wang, Huiling Chen, Bo Yang, Xuehua Zhao, Lufeng Hu, ZhenNao Cai, Hui Huang, Changfei Tong, Toward an optimal kernel extreme learning machine

using a chaotic moth-flame optimization strategy with applications in medical diagnoses, Neurocomputing 267 (2017) 69–84.
[49] Guo-Qiang Zeng, Jie Chen, Yu-Xing Dai, Li-Min Li, Chong-Wei Zheng, Min-Rong, Design of fractional order pid controller for automatic regulator voltage system based on multi-objective extremal optimization, Neurocomputing 160 (2015) 173–184.
[50] Guo-Qiang Zeng, Kang-Di Lu, Yu-Xing Dai, Zheng-Jiang Zhang, Min-Rong Chen, Chong-Wei Zheng, Di Wu, Wen-Wen, Binary-coded extremal optimization for the design of pid controllers, Neurocomputing 138 (2014) 180–188.
[51] Guo-Qiang Zeng, Xiao-Qing Xie, Min-Rong Chen, Jian Weng, Adaptive population extremal optimization-based pid neural network for multivariable nonlinear control systems, Swarm and Evolutionary Computation 44 (2019) 320–334.
[52] W. Deng, J. Xu, H. Zhao, Y. Song, A novel gate resource allocation method using improved pso-based qea, in: IEEE Transactions On Intelligent Transportation Systems, Page, 2020, https://doi.org/10.1109/TITS.2020.3025796.
[53] W. Deng, J.J. Xu, Y.J. Song, H.M. Zhao, An effective improved co-evolution ant colony optimization algorithm with multi-strategies and its application, International Journal of Bio-Inspired Computation, page 16 (3) (2020) 158–170.
[54] Jiao Hu, Huiling Chen, Ali Asghar Heidari, Mingjing Wang, Xiaoqin Zhang, Ying Chen, Zhifang Pan, Orthogonal learning covariance matrix for defects of grey wolf optimizer: insights, balance, diversity, and feature selection, Knowl. Base Syst. 213 (2021) 106684.
[55] Qiang Li, Huiling Chen, Hui Huang, Xuehua Zhao, ZhenNao Cai, Changfei Tong, Wenbin Liu, Xin Tian, An enhanced grey wolf optimization based feature selection wrapped kernel extreme learning machine for medical diagnosis, Computational and Mathematical Methods in Medicine (2017) 2017.
[56] Tong Liu, Liang Hu, Chao Ma, Zhi-Yan Wang, Hui-Ling Chen, A fast approach for detection of erythemato-squamous diseases based on extreme learning machine with maximum relevance minimum redundancy feature selection, Int. J. Syst. Sci. 46 (5) (2015) 919–931.
[57] Xiang Zhang, Yueting Xu, Caiyang Yu, Ali Asghar Heidari, Shimin Li, Huiling Chen, Chengye Li, Gaussian mutational chaotic fruit fly-built optimization and feature selection, Expert Syst. Appl. 141 (2020) 112976.
[58] Yanan Zhang, Renjing Liu, Xin Wang, Huiling Chen, Chengye Li, Boosted binary harris hawks optimizer and feature selection, Eng. Comput. (2020) 1–30.
[59] Lufeng Hu, Huaizhong Li, Zhennao Cai, Feiyan Lin, Guangliang Hong, Huiling Chen, Zhongqiu Lu, A new machine-learning method to prognosticate paraquat poisoned patients by combining coagulation, liver, and kidney indices, PloS One 12 (10) (2017) e0186427.
[60] Hui Huang, Suying Zhou, Jionghui Jiang, Huiling Chen, Yuping Li, Chengye Li, A new fruit fly optimization algorithm enhanced support vector machine for diagnosis of breast cancer based on high-level features, BMC Bioinf. 20 (8) (2019) 1–14.
[61] Chengye Li, Lingxian Hou, Bishundat Yanesh Sharma, Huaizhong Li, ChengShui Chen, Yuping Li, Xuehua Zhao, Hui Huang, Zhennao Cai, Huiling Chen, Developing a new intelligent system for the diagnosis of tuberculous pleural effusion, Comput. Methods Progr. Biomed. 153 (2018) 211–225.
[62] Xuehua Zhao, Xiang Zhang, Zhennao Cai, Xin Tian, Xianqin Wang, Ying Huang, Huiling Chen, Lufeng Hu, Chaos enhanced grey wolf optimization wrapped elm for diagnosis of paraquat-poisoned patients, Comput. Biol. Chem. 78 (2019) 481–490.
[63] Xuehua Zhao, Daoliang Li, Bo Yang, Huiling Chen, Xinbin Yang, Chenglong Yu, Shuangyin Liu, A two-stage feature selection method with its application, Comput. Electr. Eng. 47 (2015) 114–125.
[64] Xuehua Zhao, Daoliang Li, Bo Yang, Chao Ma, Yungang Zhu, Huiling Chen, Feature selection based on improved ant colony optimization for online detection of foreign fiber in cotton, Appl. Soft Comput. 24 (2014) 585–596.
[65] Aiju Lin, Quanquan Wu, Ali Asghar Heidari, Yueting Xu, Huiling Chen, Wujun Geng, Chengye Li, Predicting intentions of students for master programs using a chaos-induced sine cosine-based fuzzy k-nearest neighbor classifier, Ieee Access 7 (2019) 67235–67248.
[66] Jixia Tu, Aiju Lin, Huiling Chen, Yuping Li, Chengye Li, Predict the entrepreneurial intention of fresh graduate students based on an adaptive support vector machine framework, Math. Probl Eng. 1–16 (2019) 2019.
[67] Yan Wei, Huijing Lv, Mengxiang Chen, Mingjing Wang, Ali Asghar Heidari, Huiling Chen, Chengye Li, Predicting entrepreneurial intention of students: an extreme learning machine with Gaussian barebone harris hawks optimizer, IEEE Access 8 (2020) 76841–76855.
[68] Yan Wei, Ni Ni, Dayou Liu, Huiling Chen, Mingjing Wang, Qiang Li, Xiaojun Cui, Haipeng Ye, An improved grey wolf optimization strategy enhanced svm and its application in predicting the second major, Math. Probl Eng. 1–12 (2017) 2017.
[69] Wei Zhu, Chao Ma, Xuehua Zhao, Mingjing Wang, Ali Asghar Heidari, Huiling Chen, Chengye Li, Evaluation of sino foreign cooperative education project using orthogonal sine cosine optimized kernel extreme learning machine, IEEE Access 8 (2020) 61107–61123.
[70] Jiaze Tu, Huiling Chen, H. Gandomi Amir, Mingjing Wang. Colony predation algorithm, Jounal of Bionic Engineering, 2021, pp. 674–710.
[71] Seyedali Mirjalili, Ibrahim Aljarah, Majdi Mafarja, Ali Asghar Heidari, Hossam Faris, Grey wolf optimizer: theory, literature review, and application in computational fluid dynamics problems, Nature-inspired optimizers (2020) 87–105.
[72] Seyedali Mirjalili, Moth-flame optimization algorithm: a novel nature-inspired heuristic paradigm, Knowl. Base Syst. 89 (2015) 228–249.
[73] Guang-Bin Huang, Qin-Yu Zhu, Chee-Kheong Siew, Extreme learning machine: theory and applications, Neurocomputing 70 (1–3) (2006) 489–501.
[74] Guang-Bin Huang, Hongming Zhou, Xiaojian Ding, Rui Zhang, Extreme learning machine for regression and multiclass classification, IEEE Transactions on Systems, Man, and Cybernetics, Part B (Cybernetics) 42 (2) (2011) 513–529.
[75] Sudarshan K Dhall, Chung Laung Liu, On a real-time scheduling problem, Oper. Res. 26 (1) (1978) 127–140.
[76] Amir Mohammad Fathollahi-Fard, Abbas Ahmadi, Fariba Goodarzian, Naoufel Cheikhrouhou, A bi-objective home healthcare routing and scheduling problem considering patients' satisfaction in a fuzzy environment, Appl. Soft Comput. 93 (2020) 106385.
[77] Jun-qing Li, Jia-wen Deng, Cheng-you Li, Yu-yan Han, Jie Tian, Biao Zhang, Cun-gang Wang, An improved jaya algorithm for solving the flexible job shop scheduling problem with transportation and setup times, Knowl. Base Syst. 200 (2020) 106032.
[78] Khalid S Essa, Yves Géraud, Parameters estimation from the gravity anomaly caused by the two-dimensional horizontal thin sheet applying the global particle swarm algorithm, J. Petrol. Sci. Eng. 193 (2020) 107421.
[79] G. Thippa Reddy, M. Praveen Kumar Reddy, Kuruva Lakshmanna, Dharmendra Singh Rajput, Rajesh Kaluri, Gautam Srivastava, Hybrid genetic algorithm and a fuzzy logic classifier for heart disease diagnosis, Evolutionary Intelligence 13 (2) (2020) 185–196.
[80] James Kennedy, Russell Eberhart, Particle swarm optimization, in: *Proceedings Of ICNN'95-international Conference on Neural Networks*, Volume 4, IEEE, 1995, pp. 1942–1948.
[81] Darrell Whitley, A genetic algorithm tutorial, Stat. Comput. 4 (2) (1994) 65–85.
[82] Seyedeh Zahra Mirjalili, Seyedali mirjalili, shahrzad saremi, hossam faris, and ibrahim aljarah. Grasshopper optimization algorithm for multi-objective optimization problems, Appl. Intell. 48 (4) (2018) 805–820.
[83] Ali Asghar Heidari, Seyedali mirjalili, hossam faris, ibrahim aljarah, majdi mafarja, and huiling chen. Harris hawks optimization: algorithm and applications, Future Generat. Comput. Syst. 97 (2019) 849–872.
[84] Yutao Yang, Huiling Chen, Ali Asghar Heidari, Amir H. Gandomi, Hunger games search: visions, conception, implementation, deep analysis, perspectives, and towards performance shifts, Expert Syst. Appl. 177 (2021) 114864.
[85] Quan Zou, Pengwei Xing, Leyi Wei, Bin Liu, Gene2vec: gene subsequence embedding for prediction of mammalian n6-methyladenosine sites from mrna, Rna 25 (2) (2019) 205–218.
[86] Zhihan Lv, Liang Qiao, Jinhua Li, Houbing Song, Deep-learning-enabled security issues in the internet of things, IEEE Internet of Things Journal 8 (12) (2020) 9531–9538.
[87] Zhihan Lv, Liang Qiao, Amit Kumar Singh, Qingjun Wang, Fine-grained visual computing based on deep learning, ACM Trans. Multimed Comput. Commun. Appl 17 (1s) (2021) 1–19.
[88] Xiao Cai, Jun Wang, Shouming Zhong, Kaibo Shi, Yiqian Tang, Fuzzy quantized sampled-data control for extended dissipative analysis of t–s fuzzy system and its application to wpgss, J. Franklin Inst. 358 (2) (2021) 1350–1375.
[89] Mingjing Wang, Huiling Chen, Chaotic multi-swarm whale optimizer boosted support vector machine for medical diagnosis, Appl. Soft Comput. 88 (2020) 105946.
[90] Ali W. Mohamed, Anas A. Hadi, Anas M. Fattouh, Kamal M. Jambi, Lshade with semi-parameter adaptation hybrid with cma-es for solving cec 2017 benchmark problems, in: 2017 IEEE Congress on Evolutionary Computation (CEC), IEEE, 2017, pp. 145–152.
[91] Rohit Salgotra, Urvinder Singh, Sriparna Saha, Improved cuckoo search with better search capabilities for solving cec2017 benchmark problems, in: 2018 IEEE Congress on Evolutionary Computation (CEC), IEEE, 2018, pp. 1–7.
[92] Sen Qiu, Zhelong Wang, Hongyu Zhao, Huosheng Hu, Using distributed wearable sensors to measure and evaluate human lower limb motions, IEEE Transactions on Instrumentation and Measurement 65 (4) (2016) 939–950.
[93] Chen Yang, Haishi Zhao, Lorenzo Bruzzone, Jon Atli Benediktsson, Yanchun Liang, Bin Liu, Xingguo Zeng, Renchu Guan, Chunlai Li, Ziyuan Ouyang, Lunar impact crater identification and age estimation with chang'e data by deep and transfer learning, Nat. Commun. 11 (1) (2020) 6358.
[94] Lei Jin, Zhijie Wen, Zhongyi Hu, Topology-preserving nonlinear shape registration on the shape manifold, Multimed. Tool. Appl. (2020) 1–13.
[95] Xia Wu, Xueyuan Xu, Jianhong Liu, hailing wang, bin hu, feiping transactions on neural networks nie, and learning systems. Supervised feature selection with orthogonal regression and feature weighting, IEEE Transactions on Neural Networks and Learning Systems (2020) 2991336, https://doi.org/10.1109/TNNLS.
[96] Xupeng Wang, Mohammed Bennamoun, Ferdous Sohel, Hang Lei, Diffusion geometry derived keypoints and local descriptors for 3d deformable shape analysis, J. Circ. Syst. Comput. 30 (1) (2021) 2150016.
[97] Xupeng Wang, Ferdous Sohel, Mohammed Bennamoun, Yulan Guo, Hang Lei, Scale space clustering evolution for salient region detection on 3d deformable shapes, Pattern Recogn. 71 (2017) 414–427.
[98] H. Pei, B. Yang, J. Liu, K. Chang, Active surveillance via group sparse bayesian learning, IEEE Trans. Pattern Anal. Mach. Intell. (2020) 3023092, https://doi.org/10.1109/TPAMI.
[99] X. Xue, Z. Chen, S. Wang, Z. Feng, Y. Duan, Z. Zhou, Value entropy: a systematic evaluation model of service ecosystem evolution, IEEE Transactions on Services Computing (2020) 3016660, https://doi.org/10.1109/TSC.
[100] X. Xue, S.F. Wang, L.J. Zhan, Z.Y. Feng, Y.D. Guo, Social learning evolution (sle): computational experiment-based modeling framework of social manufacturing, Ieee Transactions on Industrial Informatics 15 (6) (2019) 3343–3355.

[101] Jingting Li, Catherine Soladie, Renaud Seguier, Local temporal pattern and data augmentation for micro-expression spotting, IEEE Transactions on Affective Computing (2020) 3023821, https://doi.org/10.1109/TAFFC.
[102] Su-Jing Wang, Ying He, Jingting Li, Xiaolan Fu, Mesnet: a convolutional neural network for spotting multi-scale micro-expression intervals in long videos, IEEE Trans. Image Process. 30 (2021) 3956–3969.
[103] Yue Yang, Hanli Zhao, Lihua You, Renlong Tu, Xueyi Wu, Xiaogang Multimedia Tools Jin, Applications, Semantic portrait color transfer with internet images, Multimed. Tool. Appl. 76 (1) (2017) 523–541.
[104] Hanli Zhao, Heyang Guo, Xiaogang Jin, Jianbing Shen, Xiaoyang Mao, Junru, Parallel and efficient approximate nearest patch matching for image editing applications, Neurocomputing 305 (2018) 39–50.
[105] Yandan Zhao, Xiaogang jin, yingqing xu, hanli zhao, meng ai, kun transactions on visualization Zhou, and computer graphics. Parallel style-aware image cloning for artworks, IEEE Trans. Visual. Comput. Graph. 21 (2) (2014) 229–240.
[106] Abdoul Fatakhou Ba, Hui Huang, Mingjing Wang, Xiaojia Ye, Zhiyang Gu, Huiling Chen, Xueding Cai, Levy-based antlion-inspired optimizers with orthogonal learning scheme. *Engineering with Computers*, pages 10.1007/s00366–020–01042–7, 2020.
[107] Xi Liang, Zhennao Cai, Mingjing Wang, Xuehua Zhao, Huiling Chen, Chengye Li Chaotic, Oppositional sine–cosine method for solving global optimization problems. *Engineering with Computers*, pages 10.1007/s00366–020–01083–y, 2020.
[108] Chunliang Feng, Zhiyuan Zhu, Zaixu Cui, Vadim Ushakov, Jean-Claude Dreher, Wenbo Luo, Ruolei Gu, Xia Wu, Frank Krueger, Prediction of trust propensity from intrinsic brain morphology and functional connectome, Hum. Brain Mapp. 42 (1) (2021) 175–191.
[109] Hechang Chen, Bo Yang, Liu Jiming, Zhou Xiao-Nong, S. Yu Philip, Mining spatiotemporal diffusion network: a new framework of active surveillance planning, IEEE Access 7 (2019) 108458–108473.
[110] Hechang Chen, Bo Yang, Hongbin Pei, Jiming Liu, Next generation technology for epidemic prevention and control: data-driven contact tracking, Ieee Access 7 (2018) 2633–2642.
[111] Xueyan Liu, Bo Yang, Hechang Chen, Katarzyna Musial, Hongxu Chen, Yang Li, Wanli Zuo, A scalable redefined stochastic blockmodel, ACM Trans. Knowl. Discov. Data 15 (3) (2021) 1–28.
[112] Xiaoyu Cao, Tianxiang Cao, Feng Gao, Xiaohong Guan, Risk-averse storage planning for improving res hosting capacity under uncertain siting choice, IEEE Transactions on Sustainable Energy (2021) 3075615, https://doi.org/10.1109/TSTE.
[113] Pengcheng Huang, Li Zhao, Runhua Jiang, Tao Wang, Xiaoqin Zhang, Self-filtering image dehazing with self-supporting module, Neurocomputing 432 (2021) 57–69.
[114] Tao Wang, Li Zhao, Pengcheng Huang, Xiaoqin Zhang, Jiawei Xu, Haze concentration adaptive network for image dehazing, Neurocomputing 439 (2021) 75–85.
[115] Xiaoqin Zhang, Tao Wang, Jinxin Wang, Guiying Tang, Li Zhao Pyramid, channel-based feature attention network for image dehazing, Comput. Vis. Image Understand. 197–198 (2020) 103003.
[116] Jun Li, Chaochao Chen, Huiling Chen, Changfei Tong, Towards context-aware social recommendation via individual trust, Knowl. Base Syst. 127 (2017) 58–66.
[117] Jun Li, Jian Lin, A probability distribution detection based hybrid ensemble qos prediction approach, Inf. Sci. 519 (2020) 289–305.
[118] Jun Li, Xiao-Lin Zheng, Song-Tao Chen, William-Wei Song, De-ren Chen, An efficient and reliable approach for quality-of-service-aware service composition, Inf. Sci. 269 (2014) 238–254.
[119] C. Chen, Qi Wu, Z. Li, Lei Xiao, Zhong Yi Hu, Diagnosis of alzheimer's disease based on deeply-fused nets, Comb. Chem. High Throughput Screen. 24(6) (2020) 781–789.
[120] Xiaoyan Fei, Jun Wang, Shihui Ying, Zhongyi Hu, Jun Shi, Projective parameter transfer based sparse multiple empirical kernel learning machine for diagnosis of brain disease, Neurocomputing 413 (2020) 271–283.
[121] Zhongyi Hu, Jun Wang, Chunxiang Zhang, Zhenzhen Luo, Xiaoqing Luo, Lei Xiao, Jun Shi, Uncertainty modeling for multi center autism spectrum disorder classification using takagi-sugeno-kang fuzzy systems, IEEE Transactions on Cognitive and Developmental Systems (2021), https://doi.org/10.1109/TCDS.2021.3073368.
[122] A. Saber, M. Sakr, O.M. Abo-Seida, A. Keshk, H. Chen, A novel deep-learning model for automatic detection and classification of breast cancer using the transfer-learning technique, IEEE Access 9 (2021) 71194–71209.
[123] L. Zhang, Z. Zhang, W. Wang, Z. Jin, Y. Su, H. Chen, Research on a covert communication model realized by using smart contracts in blockchain environment, IEEE Systems Journal, page 10.1109/JSYST (2021) 3057333.
[124] Lejun Zhang, Zhijie Zhang, Weizheng Wang, Rasheed Waqas, Chunhui Zhao, Seokhoon Kim, Huiling Chen, A covert communication method using special bitcoin addresses generated by vanitygen, Comput. Mater. Continua (CMC) 65 (1) (2020) 597–616.
[125] Sen Qiu, Zhelong Wang, Hongyu Zhao, Kairong Qin, Zhenglin Li, Huosheng Hu, Inertial/magnetic sensors based pedestrian dead reckoning by means of multi-sensor fusion, Inf. Fusion 39 (2018) 108–119.
[126] Mingyu Fan, Xiaoqin Zhang, Jie Hu, Nannan Gu, Dacheng Tao, Adaptive data structure regularized multiclass discriminative feature selection, IEEE Transactions on Neural Networks and Learning Systems (2021), https://doi.org/10.1109/TNNLS.2021.3071603.
[127] Xiaoqin Zhang, Mingyu Fan, Di Wang, Peng Zhou, Dacheng Tao, Top-k feature selection framework using robust 0-1 integer programming, IEEE Transactions on Neural Networks and Learning Systems 32 (7) (2020) 3005–3019.
[128] Xiaoqin Zhang, Wei Li, Xiuzi Ye, Stephen Maybank, Robust hand tracking via novel multi-cue integration, Neurocomputing 157 (2015) 296–305.
[129] Carol P. Chong, Philip R. Street, Pneumonia in the elderly: a review of the epidemiology, pathogenesis, microbiology, and clinical features, South. Med. J. 101 (11) (2008) 1141–1145.
[130] Jun Shu, Pneumonia in the elderly: understanding the characteristics, South. Med. J. 101 (11) (2008) 1086, 1086.
[131] Maimuna S. Majumder, Sheryl A. Kluberg, Sumiko R. Mekaru, John S. Brownstein, Mortality risk factors for middle east respiratory syndrome outbreak, South Korea, Emerg. Infect. Dis. 21 (11) (2015), 2088, 2015.
[132] Ki-Ho Hong, Jae-Phil Choi, Seon-Hui Hong, Jeewon Lee, Ji-Soo Kwon, Sun-Mi Kim, Se Yoon Park, Ji-Young Rhee, Baek-Nam Kim, Hee Jung Choi, et al., Predictors of mortality in middle east respiratory syndrome (mers), Thorax 73 (3) (2018) 286–289.
[133] Kin Wing Choi, Tai Nin Chau, Owen Tsang, Eugene Tso, Ming Chee Chiu, Wing Lok Tong, Po Oi Lee, Tak Keung Ng, Wai Fu Ng, Kam Cheong Lee, et al., Outcomes and prognostic factors in 267 patients with severe acute respiratory syndrome in Hong Kong, Ann. Intern. Med. 139 (9) (2003) 715–723.
[134] Dawei Wang, Bo Hu, Chang Hu, Fangfang Zhu, Xing Liu, Jing Zhang, Binbin Wang, Hui Xiang, Zhenshun Cheng, Yong Xiong, et al., Clinical characteristics of 138 hospitalized patients with 2019 novel coronavirus–infected pneumonia in wuhan, China, Jama 323 (11) (2020) 1061–1069.
[135] Fei Zhou, Ting Yu, Ronghui Du, Guohui Fan, Ying Liu, Zhibo Liu, Jie Xiang, Yeming Wang, Bin Song, Xiaoying Gu, et al., Clinical course and risk factors for mortality of adult inpatients with covid-19 in wuhan, China: a retrospective cohort study, The lancet 395 (10229) (2020) 1054–1062.
[136] Joseph T. Wu, Kathy Leung, Mary Bushman, Nishant Kishore, Rene Niehus, Pablo M. de Salazar, Benjamin J. Cowling, Marc Lipsitch, Gabriel M. Leung, Estimating clinical severity of covid-19 from the transmission dynamics in wuhan, China, Nat. Med. 26 (4) (2020) 506–510.
[137] Marc E. Weksler, Changes in the b-cell repertoire with age, Vaccine 18 (16) (2000) 1624–1628.
[138] Daniela Weiskopf, Birgit Weinberger, Beatrix Grubeck-Loebenstein, The aging of the immune system, Transpl. Int. 22 (11) (2009) 1041–1050.
[139] Steven M. Opal, Timothy D. Girard, E. Wesley Ely, The immunopathogenesis of sepsis in elderly patients, Clin. Infect. Dis. 41 (Supplement_7) (2005) S504–S512.
[140] Jung Yeon Heo, Joon Young Song, Ji Yun Noh, Min Joo Choi, Jin Gu Yoon, Saem Na Lee, Hee Jin Cheong, Woo Joo Kim, Effects of influenza immunization on pneumonia in the elderly, Hum. Vaccines Immunother. 14 (3) (2018) 744–749.
[141] Kui Liu, Yuan-Yuan Fang, Yan Deng, Wei Liu, Mei-Fang Wang, Jing-Ping Ma, Wei Xiao, Ying-Nan Wang, Min-Hua Zhong, Cheng-Hong Li, et al., Clinical characteristics of novel coronavirus cases in tertiary hospitals in hubei province, Chinese medical journal 133 (9) (2020) 1025.
[142] L. Zhou, H.G. Liu, Early detection and disease assessment of patients with novel coronavirus pneumonia, Zhonghua jie he he hu xi za zhi= Zhonghua Jiehe he Huxi Zazhi= Chinese Journal of Tuberculosis and Respiratory Diseases 43 (2020). E003–E003.
[143] Tai-Nin Chau, Kam-Cheong Lee, Hung Yao, Tak-Yin Tsang, Tat-Chong Chow, Yiu-Cheong Yeung, Kin-Wing Choi, Yuk-Keung Tso, Terence Lau, Sik-To Lai, et al., Sars-associated viral hepatitis caused by a novel coronavirus: report of three cases, Hepatology 39 (2) (2004) 302–310.
[144] Khaled O. Alsaad, Ali H. Hajeer, Mohammed Al Balwi, Mohammed Al Moaiqel, Nourah Al Oudah, Abdulaziz Al Ajlan, Sameera AlJohani, Sami Alsolamy, Giamal E. Gmati, Hanan Balkhy, et al., Histopathology of middle east respiratory syndrome coronovirus (mers-cov) infection–clinicopathological and ultrastructural study, Histopathology 72 (3) (2018) 516–524.
[145] Heshui Shi, Xiaoyu Han, Nanchuan Jiang, Yukun Cao, Osamah Alwalid, Jin Gu, Yanqing Fan, Chuansheng Zheng, Radiological findings from 81 patients with covid-19 pneumonia in wuhan, China: a descriptive study, Lancet Infect. Dis. 20 (4) (2020) 425–434.
[146] Nanshan Chen, Min Zhou, Xuan Dong, Jieming Qu, Fengyun Gong, Yang Han, Yang Qiu, Jingli Wang, Ying Liu, Yuan Wei, et al., Epidemiological and clinical characteristics of 99 cases of 2019 novel coronavirus pneumonia in wuhan, China: a descriptive study, The lancet 395 (10223) (2020) 507–513.
[147] Chan-Ho Lee, Sang-Won Park, Yeong Shik Kim, Sam Sik Kang, Jeong Ah Kim, Seung Ho Lee, Sun-Mee Lee, Protective mechanism of glycyrrhizin on acute liver injury induced by carbon tetrachloride in mice, Biol. Pharm. Bull. 30 (10) (2007) 1898–1904.
[148] Stef J. Koppelman, Shyamali Jayasena, Dion Luykx, Erik Schepens, Danijela Apostolovic, Govardus AH. De Jong, Thomas G. Isleib, Julie Nordlee, Joe Baumert, Steve L. Taylor, et al., Allergenicity attributes of different peanut market types, Food Chem. Toxicol. 91 (2016) 82–90.
[149] Chaolin Huang, Yeming Wang, Xingwang Li, Lili Ren, Jianping Zhao, Yi Hu, Li Zhang, Guohui Fan, Jiuyang Xu, Xiaoying Gu, et al., Clinical features of patients infected with 2019 novel coronavirus in wuhan, China, The lancet 395 (10223) (2020) 497–506.
[150] Zhe Xu, Lei Shi, Yijin Wang, Jiyuan Zhang, Lei Huang, Chao Zhang, Shuhong Liu, Peng Zhao, Hongxia Liu, Li Zhu, et al., Pathological findings of covid-19 associated with acute respiratory distress syndrome, The Lancet respiratory medicine 8 (4) (2020) 420–422.
[151] Mustafa Ahmed Abdel-Reheim, Basim Anwar Shehata Messiha, and Ali Ahmed Abo-Saif. Quillaja saponaria bark saponin protects wistar rats against ferrous

sulphate-induced oxidative and inflammatory liver damage, Pharmaceut. Biol. 55 (1) (2017) 1972–1983.
[152] Xiao-Liang Shu, Kai Kang, Li-Juan Gu, Yong-Sheng Zhang, Effect of early enteral nutrition on patients with digestive tract surgery: a meta-analysis of randomized controlled trials, Experimental and therapeutic medicine 12 (4) (2016) 2136–2144.
[153] Yanjun He, Miaogen Li, Caiyuan Mai, Lujing Chen, Xiaoman Zhang, Jianyong Zhou, Zhiguo Yang, Jia Ni, Yongxing Chen, Mian Cai, et al., Anemia and low albumin levels are associated with severe community-acquired pneumonia in pregnancy: a case-control study, Tohoku J. Exp. Med. 248 (4) (2019) 297–305.
[154] Jae Hyuk Lee, Jooyeong Kim, Kyuseok Kim, You Hwan Jo, JoongEui Rhee, Tae Youn Kim, Sang Hoon Na, Seung Sik Hwang, Albumin and c-reactive protein have prognostic significance in patients with community-acquired pneumonia, J. Crit. Care 26 (3) (2011) 287–294.
[155] Wei Liu, Zhao-Wu Tao, Lei Wang, Ming-Li Yuan, Kui Liu, Ling Zhou, Shuang Wei, Yan Deng, Jing Liu, Hui-Guo Liu, et al., Analysis of factors associated with disease outcomes in hospitalized patients with 2019 novel coronavirus disease, Chinese medical journal 133 (9) (2020) 1032.
[156] Jixiang Zhang, Xiaoli Wang, Xuemei Jia, Jiao Li, Ke Hu, Guozhong Chen, Jie Wei, Zuojiong Gong, Chenliang Zhou, Hongang Yu, et al., Risk factors for disease severity, unimprovement, and mortality in covid-19 patients in wuhan, China, Clin. Microbiol. Infect. 26 (6) (2020) 767–772.
[157] Qing Zhou, Hailong Cao, Zhenjun Xu, Rongfang Lan, Xin Chen, Dongjin Wang, Wei Xu, Baseline serum globulin as a predictor of the recurrence of lone atrial fibrillation after radiofrequency catheter ablation, Anatol. J. Cardiol. 17 (5) (2017) 381.
[158] Xiao-Jing Du, Ling-Long Tang, Yan-Ping Mao, Ying Sun, Mu-Sheng Zeng, Tie-Bang Kang, Wei-Hua Jia, Ai-Hua Lin, Jun Ma, The pretreatment albumin to globulin ratio has predictive value for long-term mortality in nasopharyngeal carcinoma, PloS One 9 (4) (2014) e94473.
[159] Jinqiu Qin, Yuanyuan Qin, Yangyang Wu, Aiqiu Wei, Meiling Luo, Lin Liao, Faquan Lin Application, Of albumin/globulin ratio in elderly patients with acute exacerbation of chronic obstructive pulmonary disease, J. Thorac. Dis. 10 (8) (2018) 4923.
[160] Jose Serpa, Danish Haque, Josemon Valayam, Katharine Breaux, Maria C. Rodriguez-Barradas, Effect of combination antiretroviral treatment on total protein and calculated globulin levels among hiv-infected patients, Int. J. Infect. Dis. 14 (2010) e41–e44.
[161] Natalie M. Zahr, Peripheral tnfα elevations in abstinent alcoholics are associated with hepatitis c infection, PloS One 13 (2) (2018) e0191586.
[162] Wan-Zhi Chen, Shi-Tong Yu, Rong Xie, Yun-Xia Lv, De-Bin Xu, Ji-Chun Yu, Preoperative albumin/globulin ratio has predictive value for patients with laryngeal squamous cell carcinoma, Oncotarget 8 (29) (2017) 48240.
[163] A. Antinori, G. Maiuro, F. Pallavicini, F. Valente, G. Ventura, G. Marasca, R. Murri, E. Pizzigallo, G. Camilli, E. Tamburrini, Prognostic factors of early fatal outcome and long-term survival in patients with pneumocystis carinii pneumonia and acquired immunodeficiency syndrome, Eur. J. Epidemiol. 9 (2) (1993) 183–189.
[164] Julio SG. Montaner, Philippa H. Hawley, Juan J. Ronco, James A. Russell, Jean Quieffin, Lindsay M. Lawson, Martin T. Schechter, Multisystem organ failure predicts mortality of icu patients with acute respiratory failure secondary to aids-related pcp, Chest 102 (6) (1992) 1823–1828.
[165] Hoe-Nam Leong, Arul Earnest, Hong-Huay Lim, Chee-Fang Chin, Colin SH. Tan, Mark E. Puhaindran, Alex CH. Tan, Mark IC. Chen, Yee-Sin Leo, Sars, In Singapore-predictors of disease severity, Ann. Acad. Med. Singapore 35 (5) (2006) 326.
[166] Hsiao-Ling Chang, Kow-Tong Chen, Shu-Kuan Lai, Hung-Wei Kuo, Ih-Jen Su, Ruey S. Lin, Fung-Chang Sung, Hematological and biochemical factors predicting sars fatality in taiwan, J. Formos. Med. Assoc. 105 (6) (2006) 439–450.
[167] Zu-Li Zhang, Yu-Lei Hou, De-Tao Li, Feng-Zeng Li, Laboratory findings of covid-19: a systematic review and meta-analysis, Scand. J. Clin. Lab. Investig. 80 (6) (2020) 441–447.
[168] M. Mafarja, A.A. Heidari, H. Faris, S. Mirjalili, I. Aljarah, Dragonfly algorithm: theory, literature review, and application in feature selection, Nature-Inspired. Optim. (2020) 47–67.
[169] A. Lin, Q. Wu, A.A. Heidari, Y. Xu, H. Chen, W. Geng, C. Li, Predicting intentions of students for master programs using a chaos-induced sine cosine-based fuzzy K-nearest neighbor classifier, Ieee Access 7 (2019) 67235–67248.
[170] H. Chantar, M. Mafarja, H. Alsawalqah, A.A. Heidari, I. Aljarah, H. Faris, Feature selection using binary grey wolf optimizer with elite-based crossover for Arabic text classification, Neural. Comput. Appli. 32 (16) (2020) 12201–12220.